Published June 30, 2008

and dsRNA, in addition to 5′-triphosphate ssRNA, might be a target for RIG-I–mediated recognition in vivo. On the other hand, long dsRNA could be generated in EMCV-infected cells and recognized by MDA5. Next, we examined the length of dsRNA generated after VSV infection. RNA harvested from cells infected with VSV for 6 or 9 h was electrophoresed, transferred to a nylon membrane, and blotted with anti-dsRNA antibody. As shown in Fig. 6 E, a dsRNA band was detected in the RNA sample (9-h infection of VSV), and the dsRNA migrated similar to M fragment of reovirus genomic RNA, suggesting that dsRNA generated in VSV infection is 2.2 kbp. We compared the lengths of dsRNAs generated in VSV- and EMCV-infected cells. As shown in Fig. 6 E, dsRNA found in EMCV-infected cells was much longer than that detected in VSV-infected cells. Although it is di cult to determine precise length of dsRNAs, the dsRNA from EMCV-infected cells migrated much slower than the L fragment of reovirus genomic RNA (3.9 kbp). These data suggest that the lengths of dsRNAs generated in RNA virus-infected cells varied depending on the virus species, and this di erence could explain the di erential recognition of viruses by RIG-I and MDA5.

DISCUSSION

Our data indicate that RIG-I recognizes dsRNA in addition to 5′-triphosphate end ssRNA, and the length of dsRNA determines the utilization of RIG-I and MDA5 for the recognition. Genomic dsRNAs of Reovirus are also di erentially recognized by RIG-I and MDA5 depending on the length of the dsRNA. The results also indicate that VSV, a rhabdovirus recognized by RIG-I, generates dsRNA in infected cells, whereas in uenza virus does not generate dsRNA in the cells as reported previously (33).

The 5′-triphosphate ssRNA has been considered to be the sole ligand for RIG-I because dsRNA has been generated in vitro by a T7 polymerase using nucleotide-triphosphates as substrates (34). However, we discovered that RNase III-treated short poly I:C is another RIG-I ligand (Fig. 1). Poly I:C, a synthetic MDA5 ligand, was converted to a RIG-I ligand, when the length of dsRNA was shortened. The 5′ ends of short poly I:C harbor either monophosphate or diphosphate, showing that dsRNA without triphosphate is also a RIG-I ligand. RNase III and Dicer are dsRNA speci c endonucleases generating 15–25 nt short dsRNAs, which mediate RNAi in a cell. Indeed, completely digested poly I:C lost the activity to induce type I IFNs, indicating that a certain length of dsRNA is required for RIG-I–mediated recognition. It was reported that host RNA digested by RNase L could be recognized by RIG-I for inducing IFN-β (35). Although it is not clear if the RNase L-digested RNA could harbor 5′-triphosphate for activating immune cells, the length of RNA might be important for RIG-I–mediated recognition in RNA digested with RNase L. Furthermore, chemically synthesized RNAs which do not possess a phosphate at the 5′ end also stimulated cells in a RIG-I–dependent manner, clearly indicating that dsRNA elicits RIG-I–mediated IFN responses independent of 5′-triphosphate. The amount of IFN-β produced in response to synthetic 70 nt dsRNA was lower than that in response to 5′ triphosphate end ssRNA and short poly I:C. It may be possible that 70 nt dsRNA is not long enough to e ciently induce IFN-β in MEFs. Alternatively, the presence of mono- or diphosphate at the 5′ end of dsRNAs might enhance recognition by RIG-I.

We also clari ed that MDA5 and RIG-I directly distinguish between long and short dsRNAs generated by T7 polymerase in the presence of 7mG. 1 kbp dsRNAs induced IFNs in a RIG-I–dependent manner. 2 kbp dsRNAs induced IFNs even in RIG-I–de cient cells, and the induction was MDA5 dependent, showing that MDA5 preferentially recognizes long dsRNAs and RIG-I is involved in the recognition of short dsRNAs. This explains why poly I:C is an MDA5 ligand and poly I:C is shifted from being an MDA5 ligand to being a RIG-I ligand, after shortening of the length of dsRNA by RNase III treatment. Also, our data indicate that viral short and long dsRNA are also di erentially recognized by RIG-I and MDA5. Reovirus genome RNA contains several lengths of dsRNA fragments and long dsRNA fragments induced IFN production in an MDA5-dependent manner, whereas IFN induction by short dsRNAs was RIG-I dependent. These data indicate that MDA5 and RIG-I di erentiate between the lengths of dsRNA and the mechanism of how these helicases distinguish the length is an interesting issue.

Long and short poly I:C distinctly activated the ATPase activity of MDA5 and RIG-I, respectively. The ATPase activity was found to correlate with biological IFN responses triggered by these RNA helicases, suggesting that the induction of ATPase activity is the key to revealing the mechanism of how RIG-I and MDA5 recognize viral RNA and transduce signaling to downstream molecules. In addition to dsRNAs, triphosphate ssRNA activates the ATPase activity of RIG-I, but not of MDA5, suggesting that this ATPase activity is necessary not just for unwinding dsRNAs. Thus, the ATPase activity might be essential for conformational changes of these helicases to signal downstream, such as opening the CARD position masked by their helicases and RD domains. Whether this ATPase activity correlates with conformational changes of RIG-I and MDA5 remains to be determined and structural analysis of these helicases is desirable. Furthermore, we observed, with AFM, the speci c association of MDA5 with poly I:C and also of RIG-I with the short poly I:C. It is interesting that the binding of these helicases to dsRNA also correlates with the biological IFN responses triggered by these RNA helicases. The mechanism of how these two helicases distinguish the length of dsRNA, leading to the speci c binding to dsRNAs is an exciting issue for future studies.

Using *Mda5*$^{-/-}$ and *Rig-I*$^{-/-}$ mice, it has been shown that poly I:C is preferentially detected by MDA5 in inducing type I IFNs, and the contribution of RIG-I in poly I:C recognition was low (26). However, several reports showed that RIG-I was also involved in poly I:C recognition in vitro. Overexpression of RIG-I in cell lines activates an IFN-β promoter and its activation level is clearly augmented by poly

I:C stimulation. RIG-I, as well as MDA5, is shown to bind to poly I:C (23). We tested poly I:Cs purchased from several companies and found that the induction of IFNs by some poly I:Cs was impaired in *Rig-I*$^{-/-}$ cells when the size of these poly I:Cs was comparably small (unpublished data). These observations are also consistent with our conclusion that the length of poly I:C is important for the di erential recognition by RIG-I and MDA5.

Neither dsRNA nor 5′ triphosphate end RNA are present in the cytoplasm of host resting cells, and these RNA structures are the target of recognition by innate immunity. In response to RNA virus infection, dsRNA is generated in the course of viral RNA replication. However, it was also shown that dsRNA is barely present in infected cells, and 5′ triphosphate RNA was shown to be the major target of recognition. Indeed, dsRNA was not detected in in uenza virus infected cells as shown previously (33). Consistently, IFN-β production in response to RNA from in uenza virus–infected cells depended on the presence of the 5′-triphosphate end as determined by CIAP treatment. On the other hand, EMCV and VSV generated dsRNA in the cells, which were recognized by MDA5 and RIG-I, respectively. RNase III treatment of RNAs from VSV-infected cells impaired the IFN-β–inducing activity, indicating that dsRNA, generated in the course of VSV infection, contributed to RIG-I–mediated recognition. As reported previously, dsRNA generated by EMCV infection appears to be responsible for MDA5-mediated recognition. The length of dsRNA generated by VSV appeared to be close to 2.0–2.5 kbp by the immunoblot analysis with anti-dsRNA antibody. Given that the length of VSV genomic RNA is 11 kb, the dsRNA was not the replication intermediate of VSV. It has been reported that defective interfering (DI) particles are generated in VSV-infected cells, and the size of reported DI particles is 2.2 kb (36). Thus, dsRNA generated in the course of VSV replication might be derived from DI particles, although further studies are needed to clarify what is the source of the dsRNA. On the other hand, dsRNA found in EMCV–infected cells was much longer than that detected in VSV-infected cells. This long dsRNA is assumed as the replication intermediates of EMCV genomic RNA (8 kb); however, the characteristic of dsRNA generated by EMCV remains to be determined. These data suggest that MDA5 and RIG-I distinctly recognize long and short dsRNAs generated in a cell after RNA virus infection. RNA viruses recognized by RIG-I could possibly be subclassi ed based on the contribution of 5′-triphosphate end ssRNA and short dsRNA. In the future, it would be interesting to explore if the lengths of dsRNA di er between several RNA viruses recognized by RIG-I and MDA5.

In summary, we characterized the RNA molecules recognized by RIG-I and MDA5, and showed that dsRNAs di erentially induce RIG-I– and MDA5-mediated IFN responses depending on length. Viral RNAs were also di erentially recognized by RIG-I and MDA5, suggesting that the two helicases evolved for covering a broad spectrum of RNA viruses. The identi cation of the nature of dsRNA recognition will lead to the discovery of small molecules e ciently activating RIG-I and/or MDA5, and will lead to the development of novel vaccines and therapies against viral infection.

MATERIALS AND METHODS

Cells and viruses. *Mda5*$^{-/-}$ and *Rig-I*$^{-/-}$ MEFs and GM-CSF DCs were generated as previously described (26, 37). EMCV, in uenza virus, and VSV were obtained as previously described (26). Reovirus was as previously described (38).

Purification of recombinant RIG-I and MDA5. RIG-I protein was puri ed as previously described (24). For the synthesis of MDA5, 2xFlag-$MDA5_{2\text{-}1025}$ (MDA5) was expressed as a GST-fusion protein using a BaculoGold GST-Expression System (BD Biosciences). GST-MDA5 bound to Glutathione–Sepharose 4B (GE Healthcare) was eluted by digestion with AcTEV protease (Invitrogen) and passed through Ni-NTA Agarose (QIAGEN). MDA5 was further puri ed by Q-Sepharose (GE Healthcare) chromatography.

ATPase assays. ATPase assays were performed in 25 μl of ATPase reaction bu er (20 mM Tris-HCl, pH 8.0, 1.5 mM $MgCl_2$, and 1.5 mM DTT) including 1 μg of puri ed RIG-I or MDA5 protein and the indicated amounts of RNAs (tri-p-ssRNA, etc.). After a 15-min incubation at 37°C, 50 nmol of ATP was added and the mixture was further incubated at 37°C for 1 h. BIOMOL GREEN Reagent (BIOMOL) was added for 5 min, and the absorbance at 620 nm was determined.

Immunofluorescence analysis. MEFs were infected with the indicated virus for 8 h and xed with 4% paraformaldehyde. Cells were then permeabilized with 0.5% Triton X-100 dissolved in PBS. For the detection of dsRNA, the mouse monoclonal antibody J2 and Alexa Fluor 594 anti–mouse secondary antibody (Invitrogen) were used.

Sample solution for AFM imaging. RNAs and proteins were diluted with sterile puri ed water to the nal concentration of 25 ng/μl and 2.5 ng/μl, respectively. Each solution was incubated for 30 min at room temperature.

AFM imaging. 5 μl of each sample solution was dropped on freshly cleaved mica (Nilaco). After 1 min, the mica surface was rinsed with 100 μl of sterile puri ed water and dried in air. AFM observation was performed using a commercial microscope operating in the dynamic force mode (model SPI3700-SPA300; Seiko) with an Si micro-cantilever (model SI-DF20; Seiko; spring constant = 15 N/m, resonance frequency = 135 kHz) (39). AFM images were analyzed using the SPIP Metrology software package (Image Metrology).

Preparation of RNAs. Uncapped in vitro–transcribed dsRNA, capped RNAs, and 5′-triphosphate ssRNA were synthesized using a T7 RiboMAX Express RNAi System (Promega), the T7 Megascript Ultra kit (Ambion; 7mGpppG/GTP ratio of 8:1), and Silencer siRNA Construction kit (Ambion), respectively, following the manufacturers' instructions. Depending on the case, poly I:C was generated in vitro using PNPase with IDP or CDP. CIAP (TaKaRa) treatment was performed as previously described (29). Processing of poly I:C (GE Healthcare) was performed in 10 μl reaction bu er containing 2 μl of 5x bu er (siRNaseIII; TaKaRa), 2.5 mM $MgCl_2$, 10 μg of poly I:C, and 1 U of RNaseIII, for the indicated periods, and the reaction was stopped by 2 μl of 120 mM EDTA. RNase A and Bal31 (TaKaRa) treatment was performed according to the manufacturer's instructions. Chemically synthesized ssRNAs (70 base) with a 5′ hydroxyl were purchased from Gene Design, Inc.

Preparation of viral RNAs. Vero cells plated on 20 × 15-cm dishes were infected with multiplicity of infection 0.01 of reovirus. At 1 h after infection, medium was removed and replaced with DME containing 10% FCS and the cells were incubated for 2 d at 37°C. Then the supernatants were collected and centrifuged at 3,000 rpm for 15 min to remove cells for avoiding cellar

RNA contamination. The supernatants were harvested and centrifuged at 25,000 rpm for 90 min in an SW28 rotor at 4°C. The viral pellet was suspended in TRIzol reagent (Invitrogen) and RNA was extracted. 30 μg of reovirus RNA was obtained.

ELISA. The amount of dsRNA in viral-infected MEFs was determined by sandwich ELISA (30) using the mAb K1 as the capture antibody and biotinylated mAb J2 for detection, followed by streptavidin alkaline phosphatase. A 400-bp in vitro–transcribed dsRNA was used as a standard to calculate dsRNA concentrations. ELISA for IFN-β was performed as previously described (26).

dsRNA blot. RNA harvested from noninfected, VSV-, or EMCV-infected cells (20 μg) was electrophoresed in 1.5% agarose gel or 10% nondenaturing polyacrylamide gel, transferred to a nylon membrane (Hybond N+), blotted with mouse anti-dsRNA antibody (J2; English and Scienti c Consulting) and visualized with an enhanced chemiluminescence system (PerkinElmer). Reovirus genome RNAs were electrophoresed in the same gel and indicated as the size control.

Online supplemental material. Fig. S1 shows IFN-β production from GM-CSF–induced WT, *RIG-I*$^{-/-}$, and *MDA5*$^{-/-}$ cDCs in the stimulation with poly I:C or short poly I:C (1 μg/ml). Fig. S2 shows IFN-β production in sera of mice 6 h after intravenous injection of 20 μg poly I:C or short poly I:C. The online version of this article is available at http://www.jem.org/cgi/content/full/jem.20080091/DC1.

The authors wish to thank Y. Fujiwara, M. Shiokawa, and N. Kitagaki for technical assistance and M. Hashimoto for secretarial assistance.

This work was supported in part by grants from the Ministry of Education, Culture, Sports, Science and Technology in Japan; from the Ministry of Health, Labour and Welfare in Japan; from the 21st Century Center of Excellence Program of Japan; and from the National Institutes of Health (AI070167).

The authors have no financial conflict of interests.

Submitted: 14 January 2008
Accepted: 4 June 2008

REFERENCES

1. Akira, S., S. Uematsu, and O. Takeuchi. 2006. Pathogen recognition and innate immunity. *Cell*. 124:783–801.
2. Beutler, B., C. Eidenschenk, K. Crozat, J.L. Imler, O. Takeuchi, J.A. Ho mann, and S. Akira. 2007. Genetic analysis of resistance to viral infection. *Nat. Rev. Immunol.* 7:753–766.
3. Medzhitov, R. 2007. Recognition of microorganisms and activation of the immune response. *Nature*. 449:819–826.
4. Fujita, T., K. Onoguchi, K. Onomoto, R. Hirai, and M. Yoneyama. 2007. Triggering antiviral response by RIG-I-related RNA helicases. *Biochimie*. 89:754–760.
5. Alexopoulou, L., A.C. Holt, R. Medzhitov, and R.A. Flavell. 2001. Recognition of double-stranded RNA and activation of NF-kappaB by Toll-like receptor 3. *Nature*. 413:732–738.
6. Diebold, S.S., T. Kaisho, H. Hemmi, S. Akira, and C. Reis e Sousa. 2004. Innate antiviral responses by means of TLR7-mediated recognition of single-stranded RNA. *Science*. 303:1529–1531.
7. Heil, F., H. Hemmi, H. Hochrein, F. Ampenberger, C. Kirschning, S. Akira, G. Lipford, H. Wagner, and S. Bauer. 2004. Species-speci c recognition of single-stranded RNA via toll-like receptor 7 and 8. *Science*. 303:1526–1529.
8. Hemmi, H., O. Takeuchi, T. Kawai, T. Kaisho, S. Sato, H. Sanjo, M. Matsumoto, K. Hoshino, H. Wagner, K. Takeda, and S. Akira. 2000. A Toll-like receptor recognizes bacterial DNA. *Nature*. 408:740–745.
9. Adachi, O., T. Kawai, K. Takeda, M. Matsumoto, H. Tsutsui, M. Sakagami, K. Nakanishi, and S. Akira. 1998. Targeted disruption of the MyD88 gene results in loss of IL-1- and IL-18-mediated function. *Immunity*. 9:143–150.
10. Yamamoto, M., S. Sato, H. Hemmi, K. Hoshino, T. Kaisho, H. Sanjo, O. Takeuchi, M. Sugiyama, M. Okabe, K. Takeda, and S. Akira. 2003. Role of adaptor TRIF in the MyD88-independent toll-like receptor signaling pathway. *Science*. 301:640–643.
11. Liu, Y.J. 2005. IPC: professional type 1 interferon-producing cells and plasmacytoid dendritic cell precursors. *Annu. Rev. Immunol.* 23:275–306.
12. Yoneyama, M., M. Kikuchi, T. Natsukawa, N. Shinobu, T. Imaizumi, M. Miyagishi, K. Taira, S. Akira, and T. Fujita. 2004. The RNA helicase RIG-I has an essential function in double-stranded RNA-induced innate antiviral responses. *Nat. Immunol.* 5:730–737.
13. Andrejeva, J., K.S. Childs, D.F. Young, T.S. Carlos, N. Stock, S. Goodbourn, and R.E. Randall. 2004. The V proteins of paramyxoviruses bind the IFN-inducible RNA helicase, mda-5, and inhibit its activation of the IFN-beta promoter. *Proc. Natl. Acad. Sci. USA*. 101:17264–17269.
14. Rothenfusser, S., N. Goutagny, G. Diperna, M. Gong, B.G. Monks, A. Schoenemeyer, M. Yamamoto, S. Akira, and K.A. Fitzgerald. 2005. The RNA helicase Lgp2 inhibits TLR-independent sensing of viral replication by retinoic acid-inducible gene-I. *J. Immunol.* 175:5260–5268.
15. Kawai, T., K. Takahashi, S. Sato, C. Coban, H. Kumar, H. Kato, K.J. Ishii, O. Takeuchi, and S. Akira. 2005. IPS-1, an adaptor triggering RIG-I- and Mda5-mediated type I interferon induction. *Nat. Immunol.* 6:981–988.
16. Kumar, H., T. Kawai, H. Kato, S. Sato, K. Takahashi, C. Coban, M. Yamamoto, S. Uematsu, K.J. Ishii, O. Takeuchi, and S. Akira. 2006. Essential role of IPS-1 in innate immune responses against RNA viruses. *J. Exp. Med.* 203:1795–1803.
17. Seth, R.B., L. Sun, C.K. Ea, and Z.J. Chen. 2005. Identi cation and characterization of MAVS, a mitochondrial antiviral signaling protein that activates NF-kappaB and IRF 3. *Cell*. 122:669–682.
18. Sun, Q., L. Sun, H.H. Liu, X. Chen, R.B. Seth, J. Forman, and Z.J. Chen. 2006. The speci c and essential role of MAVS in antiviral innate immune responses. *Immunity*. 24:633–642.
19. Meylan, E., J. Curran, K. Hofmann, D. Moradpour, M. Binder, R. Bartenschlager, and J. Tschopp. 2005. Cardif is an adaptor protein in the RIG-I antiviral pathway and is targeted by hepatitis C virus. *Nature*. 437:1167–1172.
20. Xu, L.G., Y.Y. Wang, K.J. Han, L.Y. Li, Z. Zhai, and H.B. Shu. 2005. VISA is an adapter protein required for virus-triggered IFN-beta signaling. *Mol. Cell*. 19:727–740.
21. Sato, M., H. Suemori, N. Hata, M. Asagiri, K. Ogasawara, K. Nakao, T. Nakaya, M. Katsuki, S. Noguchi, N. Tanaka, and T. Taniguchi. 2000. Distinct and essential roles of transcription factors IRF-3 and IRF-7 in response to viruses for IFN-alpha/beta gene induction. *Immunity*. 13:539–548.
22. Honda, K., H. Yanai, H. Negishi, M. Asagiri, M. Sato, T. Mizutani, N. Shimada, Y. Ohba, A. Takaoka, N. Yoshida, and T. Taniguchi. 2005. IRF-7 is the master regulator of type-I interferon-dependent immune responses. *Nature*. 434:772–777.
23. Yoneyama, M., M. Kikuchi, K. Matsumoto, T. Imaizumi, M. Miyagishi, K. Taira, E. Foy, Y.M. Loo, M. Gale Jr., S. Akira, et al. 2005. Shared and unique functions of the DExD/H-Box helicases RIG-I, MDA5, and LGP2 in antiviral innate immunity. *J. Immunol.* 175:2851–2858.
24. Saito, T., R. Hirai, Y.M. Loo, D. Owen, C.L. Johnson, S.C. Sinha, S. Akira, T. Fujita, and M. Gale Jr. 2007. Regulation of innate antiviral defenses through a shared repressor domain in RIG-I and LGP2. *Proc. Natl. Acad. Sci. USA*. 104:582–587.
25. Venkataraman, T., M. Valdes, R. Elsby, S. Kakuta, G. Caceres, S. Saijo, Y. Iwakura, and G.N. Barber. 2007. Loss of DExD/H box RNA helicase LGP2 manifests disparate antiviral responses. *J. Immunol.* 178:6444–6455.
26. Kato, H., O. Takeuchi, S. Sato, M. Yoneyama, M. Yamamoto, K. Matsui, S. Uematsu, A. Jung, T. Kawai, K.J. Ishii, et al. 2006. Di erential roles of MDA5 and RIG-I helicases in the recognition of RNA viruses. *Nature*. 441:101–105.
27. Loo, Y.M., J. Fornek, N. Crochet, G. Bajwa, O. Perwitasari, L. Martinez-Sobrido, S. Akira, M.A. Gill, A. Garcia-Sastre, M.G. Katze, and M. Gale Jr. 2008. Distinct RIG-I and MDA5 signaling by RNA viruses in innate immunity. *J. Virol.* 82:335–345.

28. Gitlin, L., W. Barchet, S. Gil llan, M. Cella, B. Beutler, R.A. Flavell, M.S. Diamond, and M. Colonna. 2006. Essential role of mda-5 in type I IFN responses to polyriboinosinic:polyribocytidylic acid and encephalomyocarditis picornavirus. *Proc. Natl. Acad. Sci. USA.* 103:8459–8464.
29. Hornung, V., J. Ellegast, S. Kim, K. Brzozka, A. Jung, H. Kato, H. Poeck, S. Akira, K.K. Conzelmann, M. Schlee, et al. 2006. 5′-triphosphate RNA is the ligand for RIG-I. *Science.* 314:994–997.
30. Pichlmair, A., O. Schulz, C.P. Tan, T.I. Naslund, P. Liljestrom, F. Weber, and C. Reis e Sousa. 2006. RIG-I-mediated antiviral responses to single-stranded RNA bearing 5′-phosphates. *Science.* 314:997–1001.
31. Marques, J.T., T. Devosse, D. Wang, M. Zamanian-Daryoush, P. Serbinowski, R. Hartmann, T. Fujita, M.A. Behlke, and B.R. Williams. 2006. A structural basis for discriminating between self and nonself double-stranded RNAs in mammalian cells. *Nat. Biotechnol.* 24:559–565.
32. Grunberg-Manago, M., P.J. Oritz, and S. Ochoa. 1955. Enzymatic synthesis of nucleic acidlike polynucleotides. *Science.* 122:907–910.
33. Weber, F., V. Wagner, S.B. Rasmussen, R. Hartmann, and S.R. Paludan. 2006. Double-stranded RNA is produced by positive-strand RNA viruses and DNA viruses but not in detectable amounts by negative-strand RNA viruses. *J. Virol.* 80:5059–5064.
34. Kim, D.H., M. Longo, Y. Han, P. Lundberg, E. Cantin, and J.J. Rossi. 2004. Interferon induction by siRNAs and ssRNAs synthesized by phage polymerase. *Nat. Biotechnol.* 22:321–325.
35. Malathi, K., B. Dong, M. Gale Jr., and R.H. Silverman. 2007. Small self-RNA generated by RNase L ampli es antiviral innate immunity. *Nature.* 448:816–819.
36. Pattnaik, A.K., L.A. Ball, A. LeGrone, and G.W. Wertz. 1995. The termini of VSV DI particle RNAs are su cient to signal RNA encapsidation, replication, and budding to generate infectious particles. *Virology.* 206:760–764.
37. Kato, H., S. Sato, M. Yoneyama, M. Yamamoto, S. Uematsu, K. Matsui, T. Tsujimura, K. Takeda, T. Fujita, O. Takeuchi, and S. Akira. 2005. Cell type-speci c involvement of RIG-I in antiviral response. *Immunity.* 23:19–28.
38. Connolly, J.L., and T.S. Dermody. 2002. Virion disassembly is required for apoptosis induced by reovirus. *J. Virol.* 76:1632–1641.
39. Mikamo, E., C. Tanaka, T. Kanno, H. Akiyama, G. Jung, H. Tanaka, and T. Kawai. 2005. Native polysomes of Saccharomyces cerevisiae in liquid solution observed by atomic force microscopy. *J. Struct. Biol.* 151:106–110.

LETTERS

Loss of the autophagy protein Atg16L1 enhances endotoxin-induced IL-1β production

Tatsuya Saitoh[1,3]*, Naonobu Fujita[4]*, Myoung Ho Jang[2], Satoshi Uematsu[1,3], Bo-Gie Yang[1,3], Takashi Satoh[1,3], Hiroko Omori[4], Takeshi Noda[4], Naoki Yamamoto[5], Masaaki Komatsu[6,7,8], Keiji Tanaka[6], Taro Kawai[1,3], Tohru Tsujimura[9], Osamu Takeuchi[1,3], Tamotsu Yoshimori[4,10] & Shizuo Akira[1,3]

Systems for protein degradation are essential for tight control of the inflammatory immune response[1,2]. Autophagy, a bulk degradation system that delivers cytoplasmic constituents into autolysosomes, controls degradation of long-lived proteins, insoluble protein aggregates and invading microbes, and is suggested to be involved in the regulation of inflammation[3–5]. However, the mechanism underlying the regulation of inflammatory response by autophagy is poorly understood. Here we show that Atg16L1 (autophagy-related 16-like 1), which is implicated in Crohn's disease[6,7], regulates endotoxin-induced inflammasome activation in mice. Atg16L1-deficiency disrupts the recruitment of the Atg12-Atg5 conjugate to the isolation membrane, resulting in a loss of microtubule-associated protein 1 light chain 3 (LC3) conjugation to phosphatidylethanolamine. Consequently, both autophagosome formation and degradation of long-lived proteins are severely impaired in Atg16L1-deficient cells. Following stimulation with lipopolysaccharide, a ligand for Toll-like receptor 4 (refs 8, 9), Atg16L1-deficient macrophages produce high amounts of the inflammatory cytokines IL-1β and IL-18. In lipopolysaccharide-stimulated macrophages, Atg16L1-deficiency causes Toll/IL-1 receptor domain-containing adaptor inducing IFN-β (TRIF)-dependent activation of caspase-1, leading to increased production of IL-1β. Mice lacking Atg16L1 in haematopoietic cells are highly susceptible to dextran sulphate sodium-induced acute colitis, which is alleviated by injection of anti-IL-1β and IL-18 antibodies, indicating the importance of Atg16L1 in the suppression of intestinal inflammation. These results demonstrate that Atg16L1 is an essential component of the autophagic machinery responsible for control of the endotoxin-induced inflammatory immune response.

Autophagy is a bulk degradation system, which controls the clearance and re-use of intracellular constituents, and is important for the maintenance of an amino acid pool essential for survival[3–5]. In addition, recent studies have disclosed multiple roles of autophagy in the regulation of cell death, differentiation and anti-microbial response in mammals[4,5]. Yeast genetic screening studies have identified a variety of essential components of autophagic machinery, called Atg proteins, which are phylogenetically highly conserved, and several mammalian counterparts, such as Atg5 and Atg7, have been reported[3–5]. Previously, we systematically characterized mammalian homologues of Atg proteins and identified Atg16L1 protein as an Atg5-binding protein[10]. Its coiled-coil domain, which mediates self-multimerization, is essentially required for starvation-induced autophagy in yeast, and this domain is conserved in mammalian Atg16L1 (refs 3, 10; Fig. 1a). We have proposed that the coiled-coil domain of Atg16L1 is required for the formation of an ~800 kDa high molecular weight protein complex with the Atg12-Atg5 conjugate and defines the site where LC3 (homologue of yeast Atg8) is conjugated to phosphatidylethanolamine (PE), an essential process for autophagy, by recruitment of an Atg3-LC3 intermediate to a source membrane of an autophagosome[10,11]. In addition, Atg16L1 has seven WD40 repeats at the carboxy terminus, which are absent in yeast Atg16 (ref. 10). Recent genome-wide association studies identified Atg16L1 as a candidate gene responsible for susceptibility to Crohn's disease[6,7]. However, the importance of Atg16L1 in autophagy and its role in inflammation have not been fully understood. Hence, we generated Atg16L1 mutant mice and examined the function of Atg16L1 in autophagosome formation as well as in the regulation of immune responses.

Atg16L1 mutant mice express deleted forms of Atg16L1 protein lacking the entire coiled-coil domain (Fig. 1a, b, and Supplementary Fig. 1a–c). However, such aberrant proteins do not act as dominant-negative molecules, because ectopic expression of truncated Atg16L1 protein lacking the coiled-coil domain (ΔCCD) in wild-type mouse embryonic fibroblasts (MEFs) did not interfere with autophagy (Supplementary Fig. 2a, b). Most Atg16L1-deficient mice died within 1 day of delivery, indicating that Atg16L1 is required for survival during neonatal starvation (Supplementary Fig. 1d, e). This phenotype is similar to that observed in Atg5- or Atg7-deficient mice[12,13]. Although Atg16L1 associates with Atg12-Atg5, Atg16L1 was dispensable for Atg12 conjugation to Atg5 (Fig. 1b). On the other hand, Atg16L1 was required for LC3 conjugation to PE (Fig. 1b). In Atg16L1-deficient MEFs, formation of the high molecular weight protein complex was disrupted and Atg12-Atg5 puncta were hardly observed (Fig. 1c, d, and Supplementary Fig. 3, 4a). On the other hand, GFP-Atg5 free from Atg12-conjugation formed puncta in Atg7-deficient MEFs or Atg5-deficient MEFs complemented with GFP-Atg5^{K130R}, although these puncta did not colocalize with LC3 (Fig. 1c, d, Supplementary Figs 4b, 5, data not shown). Formation of autophagosomes under the starved condition was not observed in Atg16L1-deficient MEFs, resulting in a decrease in the bulk degradation of long-lived proteins and the accumulation of p62/SQSTM1 (Fig. 1b–f). These results indicated that Atg16L1 is essentially required for autophagy by regulating the localization of the Atg12-Atg5 conjugate.

[1]Laboratory of Host Defense, [2]Laboratory of Gastrointestinal Immunology, WPI Immunology Frontier Research Center, Osaka University, 3-1 Yamada-oka, Suita, Osaka 565-0871, Japan. [3]Department of Host Defense, [4]Department of Cellular Regulation, Research Institute for Microbial Diseases, Osaka University, 3-1 Yamada-oka, Suita, Osaka 565-0871, Japan. [5]AIDS Research Center, National Institute of Infectious Diseases, Toyama 1-23-1, Shinjuku-ku, Tokyo 162-8640, Japan. [6]Laboratory of Frontier Science, Tokyo Metropolitan Institute of Medical Science, Bunkyo-ku, Tokyo 113-8613, Japan. [7]Department of Biochemistry, Juntendo University School of Medicine, 2-1-1 Hongo Bunkyo-ku, Tokyo 113-8421, Japan. [8]PRESTO, Japan Science and Technology Corporation, Kawaguchi, Saitama 332-0012, Japan. [9]Department of Pathology, Hyogo College of Medicine, 1-1 Mukogawa-cho, Nishinomiya, Hyogo 663-8501, Japan. [10]CREST, Japan Science and Technology Agency, 4-1-8 Honcho, Kawaguchi, Saitama 332-0012, Japan.
*These authors contributed equally to this work.

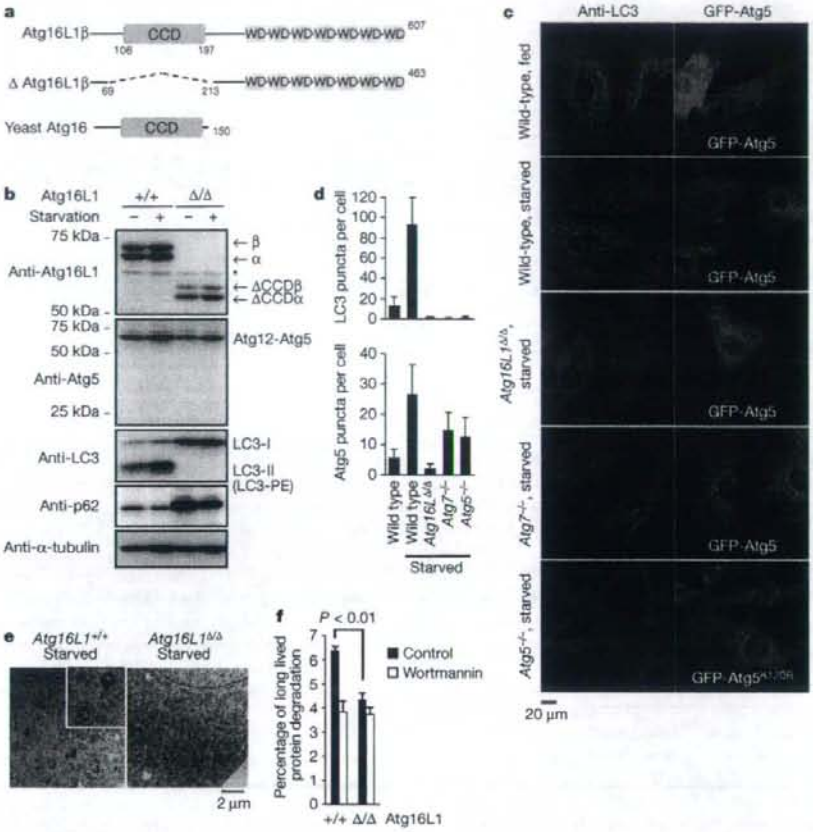

Figure 1 | Atg16L1 is essential for autophagy. a, Schematic structure of wild-type or truncated (Δ) Atg16L1 protein. CCD, Coiled-coil domain; WD, WD40 domain. Here and below, suffix α or β indicates isoform α or β. **b–d**, MEFs were cultured in nutrient-rich medium (fed) or Hanks' buffer (starved) for 1 h. Total cell lysates were prepared, and blotted with the indicated antibodies (**b**). α, β, indicate Atg16L1 isoform α, β; ΔCCD indicates Atg16L1ΔCCD; asterisk indicates a non-specific band. *Atg16L1*$^{\Delta/\Delta}$ indicates mice expressing ΔAtg16L1. The number of endogenous LC3 or GFP-Atg5 dots was counted (**c, d**). The results shown are mean + s.d. ($n > 20$). **e**, Electron micrograph of starved MEFs. **f**, Degradation of long-lived proteins in MEFs. Wortmannin is an autophagy inhibitor. The results shown are mean + s.d. Statistical significance (P value) was determined by the Student's t-test.

Although the involvement of autophagic machinery in the Toll-like receptor (TLR)-mediated antiviral response and phagocytosis have been reported[14,15], it is still unclear whether autophagy controls TLR-mediated inflammatory responses. We examined the role of Atg16L1 in the production of inflammatory cytokines, such as TNFα, IL-6 and IL-1β, in response to lipopolysaccharide (LPS), a major component of bacterial endotoxin[8]. Although both messenger RNA expression and production of TNFα, IL-6 and IFN-β were almost normal in Atg16L1-deficient fetal liver-derived macrophages, IL-1β production was highly elevated compared with that in wild-type macrophages (Fig. 2a, Supplementary Fig. 6). IL-1β mRNA synthesis was not impaired in Atg16L1-deficient macrophages, indicating that IL-1β production is enhanced at the post-transcriptional level in Atg16L1-deficient macrophages (Supplementary Fig. 6). Synthetic lipid A, an active component of LPS, also potently induced IL-1β production in Atg16L1-deficient cells (Fig. 2b). On the other hand, ectopic expression of the Atg16L1 protein lacking coiled-coil domain (ΔCCD) in RAW264.7 cells did not affect LPS-induced IL-1β production (Supplementary Fig. 2c, d). These results indicated that Atg16L1-deficiency is responsible for the elevated production of IL-1β.

We next generated chimaeric mice by transplantation of fetal liver cells into lethally irradiated CD45.1 mice to examine IL-1β production in other types of macrophage (Supplementary Fig. 7a–c). Following stimulation with LPS, peritoneal and bone-marrow macrophages deficient in Atg16L1 showed enhanced IL-1β production compared with wild-type macrophages (Supplementary Fig. 7d, e). Non-invasive Gram-negative bacteria, such as *Escherichia coli*, *Enterobacter aerogenes* and *Klebsiella pneumonia*, which are habitants in the commensal flora, also potently induced IL-1β production in Atg16L1-deficient cells (Supplementary Fig. 8a). On the other hand, the production of IL-1β and apoptosis induced by *Salmonella typhimurium*, an invasive Gram-negative bacterium, is almost normal in Atg16L1-deficient macrophages (Fig. 2c, Supplementary Fig. 9c). We also found that Atg16L1-deficient macrophages produced a high amount of IL-1β following stimulation by ATP or monosodium urate (MSU), an activator of the Nalp3 inflammasome[16,17] (Fig. 2c). Atg16L1-deficient macrophages normally produced inflammatory cytokine in response to muramyldipeptide, a ligand for NOD2 (ref. 16), indicating that Atg16L1 is not involved in signalling downstream of NOD2, whose de-regulation is also implicated in Crohn's disease[16] (Supplementary Fig. 10).

The expression levels of immature IL-1β protein following LPS stimulation in Atg16L1-deficient macrophages were almost comparable to those in wild-type cells, indicating an abnormality of post-translational regulation (Fig. 2d). Cleaved caspase-1, an activated

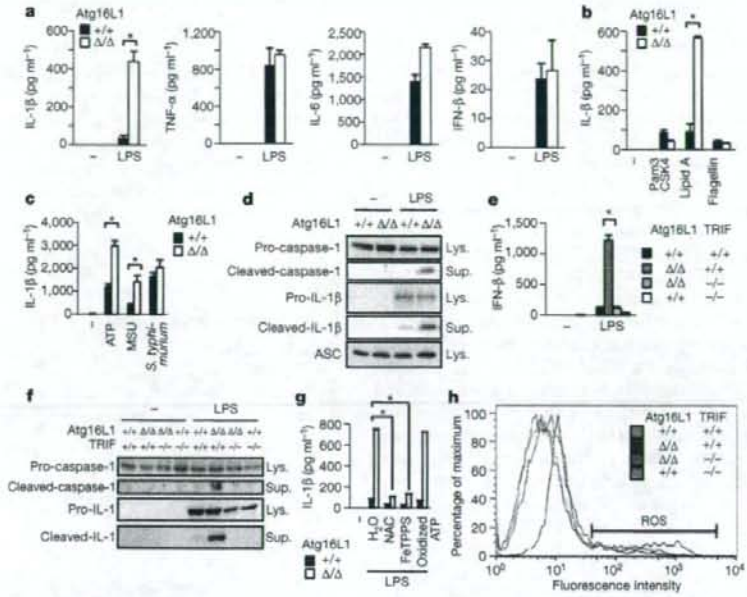

Figure 2 | Elevated endotoxin-induced IL-1β production from Atg16L1-deficient macrophages. **a**, Cytokine production from macrophages stimulated with LPS (100 ng ml^{-1}) for 24 h. Statistical significance was determined by the Student's *t*-test. $^*P < 0.01$. **b**, IL-1β production from macrophages stimulated with indicated ligands. **c**, IL-1β production from LPS-primed macrophages infected with *S. typhimurium* (multiplicity of infection, m.o.i., 1), or stimulated with ATP or MSU for 1 h. **d**, Expression levels of caspase-1 and IL-1β in macrophages. Lys., cell lysates; Sup., culture supernatants. **e**, LPS-induced production of IL-1β from macrophages with the indicated phenotype. **f**, Expression levels of caspase-1 and IL-1β in macrophages treated as in **e**. **g**, Effect of the ROS scavenger FeTPPS (25 μM), N-acetyl-L-cysteine (NAC; 25 mM) or P2X7 receptor antagonist oxidized ATP (250 μM) on IL-1β production. **h**, ROS in LPS-stimulated macrophages were detected by CM-H_2DCFDA staining.

form that mediates processing of IL-1β and apoptosis[16,17], was detected in the culture supernatants of Atg16L1-deficient macrophages following LPS stimulation, and was responsible for the production of IL-1β and the induction of apoptosis (Fig. 2d, Supplementary Figs 9a, b, 11). IL-18 production, which is regulated by caspase-1-mediated cleavage[17], was also enhanced in response to LPS in Atg16L1-deficient macrophages (Supplementary Fig. 12). Recent studies have disclosed that NF-κB and p38 signalling pathways regulate the activation of caspase-1 and the induction of cell death in macrophages stimulated with LPS[18,19]. However, activation of NF-κB, p38 and IRF-3 signalling pathways by LPS was comparable between wild-type and Atg16L1-deficient macrophages (Supplementary Fig. 13). Among TLR family members, TLR2, TLR4 and TLR5 recognize bacterial components and play important roles in the anti-bacterial response[8]. Importantly, TLR4 ligand, but not ligands for TLR2 or TLR5, induced potent IL-1β production from Atg16L1-deficient macrophages (Fig. 2b, Supplementary Fig. 14). Enhancement of IL-1β production in Atg16L1-deficient macrophages was also induced by ligands for the viral nucleotide-sensing TLRs, TLR3, TLR7 and TLR9, although the production induced by these ligands was lower than that induced by LPS (Supplementary Fig. 14).

These findings prompted us to assess the involvement of the TRIF/IFN signalling, which is strongly triggered by the engagement of TLR4 in macrophages[8] and regulates apoptosis[18]. Consistent with this hypothesis, Atg16L1/TRIF double-deficient macrophages failed

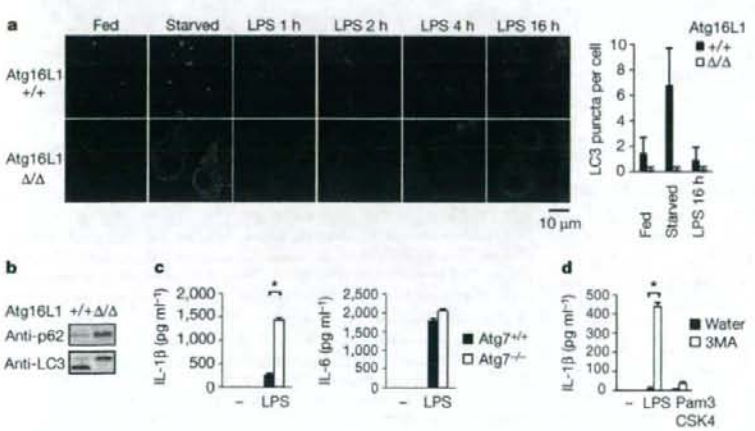

Figure 3 | Disruption of basal autophagy enhances LPS-induced IL-1β production. **a**, Macrophages were stimulated with LPS (100 ng ml^{-1}) for the indicated time period. The number of endogenous LC3 dots within each cell was counted. The results shown are mean + s.d. ($n > 100$). **b**, Expression levels of p62 and LC3 in macrophages. **c**, IL-1β and IL-6 production by wild-type or Atg7-deficient macrophages stimulated with LPS. Statistical significance was determined by the Student's *t*-test. $^*P < 0.01$. **d**, Macrophages were pre-treated with or without 10 mM 3MA and then stimulated with the indicated ligands.

to produce IL-1β due to a lack of caspase-1 activation in response to LPS (Fig. 2e, f). The simultaneous stimulation of Atg16L1-deficient macrophages with IFN-β or IFN-γ enhanced IL-1β production and apoptosis induced by TLR2 ligand (Supplementary Figs 9d, 15a). Recent studies have disclosed that K^+-efflux and reactive oxygen species (ROS), especially peroxynitrate, play important roles in the production of IL-1β induced by ATP, MSU and asbestos[16,17,20,21]. Similarly, the enhanced IL-1β production from Atg16L1-deficient macrophages required K^+-efflux and ROS generation (Fig. 2g, Supplementary Figs 15b, 16). The level of ROS in Atg16L1-deficient macrophages was higher than that in Atg16L1/TRIF double-deficient or wild-type macrophages following LPS stimulation (Fig. 2h). Oxidized ATP, an antagonist for the P2X7 receptor, did not inhibit LPS-induced IL-1β production, indicating that extracellular ATP is not involved in its production (Fig. 2g). These results indicate that loss of Atg16L1 in macrophages causes aberrant LPS-induced IL-1β production in a TRIF-dependent manner. ROS might be accumulated in Atg16L1-deficient macrophages undergoing apoptosis and trigger caspase-1 activation following LPS stimulation.

The involvement of TLR signalling in the induction of autophagy has been recently reported[22,23]. Therefore we examined if stimulation of TLR4 or other TLRs induces puncta formation by endogenous LC3. In contrast to previous reports, LPS stimulation did not increase the number of LC3 puncta in primary macrophages, although nutrient deprivation induced the formation of autophagosomes (Fig. 3a, Supplementary Fig. 17a–c). Stimulation by other ligands for TLRs also failed to increase the number of puncta of endogenous LC3 in these macrophages (Supplementary Fig. 17b, d, e). Co-incubation with non-invasive bacteria did not increase the number of autophagosomes in macrophages (Supplementary Fig. 8b). On the other hand, infection with *S. typhimurium* resulted in Atg16L1-dependent formation of bacteria autophagosomes, even in the absence of both MyD88 and TRIF, essential adaptor molecules for TLR signalling pathways[8,9] (Supplementary Fig. 18a, b). These results indicated that TLR signalling is not associated with the formation of autophagosomes in primary macrophages.

Increasing evidence has revealed that basal autophagy plays critical roles under both physiological and pathological conditions, including neurodegeneration, hepatic dysfunction and the immune response[13,24–26]. In Atg16L1-deficient macrophages, autophagosomes were hardly detected and p62/SQSTM1 protein was accumulated under nutrient-rich conditions, indicating that basal autophagy is almost completely inhibited (Fig. 3a, b). Atg7-deficient macrophages also produced high levels of IL-1β in response to LPS, but produced normal levels of IL-6 (Fig. 3c). A chemical inhibitor of autophagy, 3-methyladenine (3MA), significantly enhanced production of IL-1β from wild-type peritoneal macrophages induced by stimulation with LPS, but not with ligand for TLR2 (Fig. 3d). Macrophages treated with 3MA underwent apoptosis following LPS stimulation (Supplementary Fig. 9e). Further, transient expression of inactive mutant of Atg4B, which inhibits the LC3 lipidation, enhanced LPS-induced IL-1β production in RAW264.7 cells (Supplementary Fig. 19a, b). These results indicate that inhibition of basal autophagy induces IL-1β overproduction.

Aberrant expression of inflammatory cytokines, including IL-1β and IL-18, has been shown to be involved in the development of colitis[27,28], and recent studies have reported that Atg16L1 is a candidate susceptibility gene for Crohn's disease[6,7]. Under specific pathogen-free conditions, Atg16L1-deficient chimaeric mice did not develop spontaneous colitis, and the colons of newborn Atg16L1-deficient mice were not inflamed (Supplementary Fig. 20a, b). The number of bacteria in the faeces of wild-type or Atg16L1-deficient chimaeric mice was almost same, and no bacteria were detected in spleen (Supplementary Fig. 20c, d). The number of $CD4^+Foxp3^+$ regulatory T cells, which suppress the inflammatory response and are required for immune homeostasis[29], was almost normal in the spleens and mesenteric lymph nodes of Atg16L1-deficient chimaeric mice (Supplementary Fig. 21a, b). We next assessed if Atg16L1-deficiency exacerbates inflammation in a dextran sulphate sodium (DSS)-induced experimental model of colitis. Strikingly, all chimaeric mice with Atg16L1-deficient haematopoietic cells died together with severe body weight loss following seven days of DSS exposure, whereas all chimaeric mice expressing wild-type Atg16L1 survived (Fig. 4a, b). Histological analyses revealed much severer inflammation in the distal colons of Atg16L1-deficient mice than in wild-type controls, with larger areas of ulceration and increased infiltration of lymphocytes

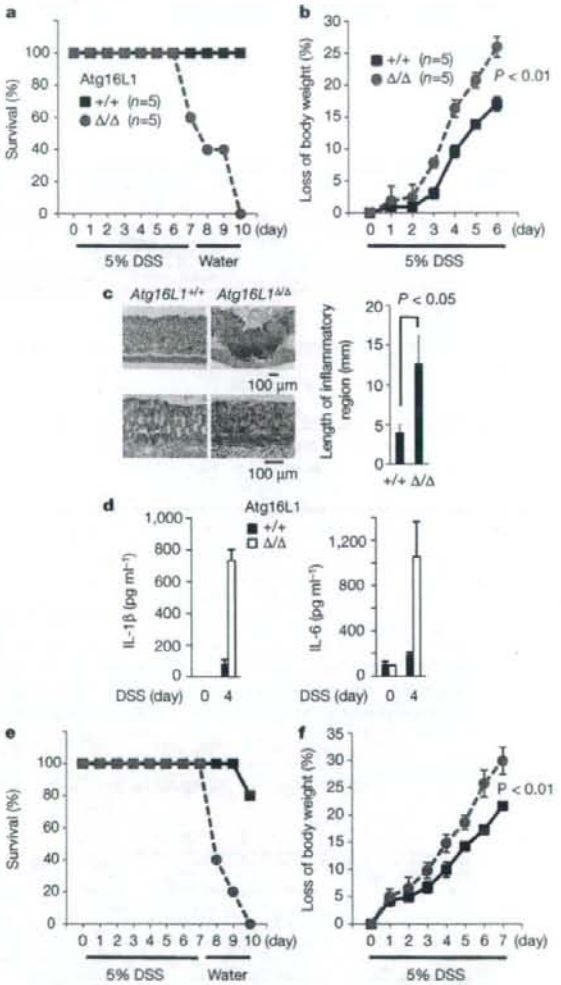

Figure 4 | Severe DSS-induced colitis in Atg16L1-deficient chimaeric mice. **a**, **b**, Fetal liver chimaeric mice were given 5% DSS in drinking water for 7 days. The survival (**a**) and weight loss (**b**) of each mouse genotype were plotted. The results shown are mean ± s.d. Statistical significance was determined by the Student's *t*-test. **c**, Typical distal colon appearance 6 days after the initiation of DSS administration. The results shown are mean ± s.d. ($n = 3$, each group). **d**, Expression levels of IL-1β and IL-18 in serum ($n = 5$, each group). **e**, **f**, Atg16L1-deficient chimaeric mice given 5% DSS in drinking water were intraperitoneally injected with both anti-IL-1β and anti-IL-18 neutralizing antibodies (squares; $n = 5$) or isotype control IgG (circles; $n = 5$) at days 1, 3, 5 and 7. The survival (**e**) and weight loss (**f**) of each mouse genotype were plotted.

(Fig. 4c). The levels of the proinflammatory cytokines IL-1β and IL-18 were significantly elevated in the sera of DSS-treated Atg16L1-deficient chimaeric mice relative to the levels in wild-type counterparts (Fig. 4d). Mortality and loss of body weight after DSS-exposure in Atg16L1-deficient chimaeric mice were improved by the injection of neutralizing antibodies for IL-1β and IL-18, showing the involvement of excessive production of these cytokines in the development of severe colitis (Fig. 4e, f). Administration of 3MA increased the level of IL-1β in serum and worsened the survival rate of mice treated with DSS, suggesting that autophagy protects mice from massive inflammation during colitis (Supplementary Fig. 22).

Our present study highlights a novel role for autophagy in the regulation of the inflammatory immune response. Autophagy controls inflammasome activation and limits production of the inflammatory cytokines IL-1β and IL-18. Given the importance of elevated expression of IL-1β and IL-18 caused by Atg16L1 deficiency in the pathology of chemical-induced colitis, it would be of interest to examine the involvement of autophagy in the pathogenesis of inflammatory bowel diseases such as Crohn's disease.

METHODS SUMMARY

Mice, reagents, cells and plasmids. Details are given in Methods.

Preparation of macrophages. E15.5 fetal liver stem cells from wild-type or Atg16L1-deficient littermates were cultured in the presence of GM-CSF (10 ng ml^{-1}) for 7 days to generate fetal liver macrophages. Unattached cells were removed on days 2, 4 and 6. Unless otherwise noted, fetal liver macrophages were used in the experiments. Bone-marrow-derived and peritoneal macrophages were prepared as described[9].

Histopathological analysis. The colon was removed and fixed with 4% PFA. The paraffin sections were stained with haematoxylin and eosin (H&E), and histologically analysed.

RT–PCR, immunoblotting, ELISA. Details of RT–PCR procedures are given in Methods. Immunoblotting was performed as described[11], and the experiments were repeated at least twice. The level of cytokine production was measured by ELISA according to the manufacturer's instructions. The results shown are means ± s.d. from three separate samples. The experiments were repeated at least three times.

Fluorescence microscopy analysis. Cells cultured on coverslips were fixed with 3% paraformaldehyde, and subjected to immunocytochemistry[11]. Samples were examined under a fluorescence laser scanning confocal FV1000 microscope (Olympus).

Detection of ROS. Macrophages were stimulated with LPS for 22 h, and then stained with CM-H_2DCFDA (10 μM; Molecular Probes), a fluorescent indicator for ROS, for 2 h. The level of fluorescence was determined by flow cytometry. The experiments were repeated at least three times.

Gel filtration, electron microscopy analysis, bulk protein degradation assay. Gel filtration analysis was performed as described[11]; electron microscopy analysis was performed as described[36]; details on the bulk protein degradation assay are given in Methods.

Full Methods and any associated references are available in the online version of the paper at www.nature.com/nature.

Received 7 August; accepted 26 August 2008.
Published online 5 October 2008.

1. Liu, Y. C., Penninger, J. & Karin, M. Immunity by ubiquitylation: A reversible process of modification. *Nature Rev. Immunol.* **5**, 941–952 (2005).
2. Wang, Y. *et al.* Lysosome-associated small Rab GTPase Rab7b negatively regulates TLR4 signaling in macrophages by promoting lysosomal degradation of TLR4. *Blood* **110**, 962–971 (2007).
3. Ohsumi, Y. Molecular dissection of autophagy: Two ubiquitin-like systems. *Nature Rev. Mol. Cell Biol.* **2**, 211–216 (2001).
4. Mizushima, N., Levine, B., Cuervo, A. M. & Klionsky, D. J. Autophagy fights disease through cellular self-digestion. *Nature* **451**, 1069–1075 (2008).
5. Levine, B. & Deretic, V. Unveiling the roles of autophagy in innate and adaptive immunity. *Nature Rev. Immunol.* **7**, 767–777 (2007).
6. Hampe, J. *et al.* A genome-wide association scan of nonsynonymous SNPs identifies a susceptibility variant for Crohn disease in ATG16L1. *Nature Genet.* **39**, 207–211 (2007).
7. Rioux, J. D. *et al.* Genome-wide association study identifies new susceptibility loci for Crohn disease and implicates autophagy in disease pathogenesis. *Nature Genet.* **39**, 596–604 (2007).
8. Akira, S., Uematsu, S. & Takeuchi, O. Pathogen recognition and innate immunity. *Cell* **124**, 783–801 (2006).
9. Yamamoto, M. *et al.* Role of adaptor TRIF in the MyD88-independent toll-like receptor signaling pathway. *Science* **301**, 640–643 (2003).
10. Mizushima, N. *et al.* Mouse Apg16L, a novel WD-repeat protein, targets to the autophagic isolation membrane with the Apg12-Apg5 conjugate. *J. Cell Sci.* **116**, 1679–1688 (2003).
11. Fujita, N., Itoh, T., Fukuda, M., Noda, T. & Yoshimori, T. The Atg16L complex specifies the site of LC3 lipidation for membrane biogenesis in autophagy. *Mol. Biol. Cell* **19**, 2092–2100 (2008).
12. Kuma, A. *et al.* The role of autophagy during the early neonatal starvation period. *Nature* **432**, 1032–1036 (2004).
13. Komatsu, M. *et al.* Impairment of starvation-induced and constitutive autophagy in Atg7-deficient mice. *J. Cell Biol.* **169**, 425–434 (2005).
14. Lee, H. K., Lund, J. M., Ramanathan, B., Mizushima, N. & Iwasaki, A. Autophagy-dependent viral recognition by plasmacytoid dendritic cells. *Science* **315**, 1398–1401 (2007).
15. Sanjuan, M. A. *et al.* Toll-like receptor signalling in macrophages links the autophagy pathway to phagocytosis. *Nature* **450**, 1253–1257 (2007).
16. Kanneganti, T. D., Lamkanfi, M. & Núñez, G. Intracellular NOD-like receptors in host defense and disease. *Immunity* **27**, 549–559 (2007).
17. Pétrilli, V., Dostert, C., Muruve, D. A. & Tschopp, J. The inflammasome: A danger sensing complex triggering innate immunity. *Curr. Opin. Immunol.* **19**, 615–622 (2007).
18. Hsu, L. C. *et al.* The protein kinase PKR is required for macrophage apoptosis after activation of Toll-like receptor 4. *Nature* **428**, 341–345 (2004).
19. Greten, F. R. *et al.* NF-κB is a negative regulator of IL-1β secretion as revealed by genetic and pharmacological inhibition of IKKβ. *Cell* **130**, 918–931 (2007).
20. Dostert, C. *et al.* Innate immune activation through Nalp3 inflammasome sensing of asbestos and silica. *Science* **320**, 674–677 (2008).
21. Hewinson, J., Moore, S. F., Glover, C., Watts, A. G. & MacKenzie, A. B. A key role for redox signaling in rapid P2X7 receptor-induced IL-1beta processing in human monocytes. *J. Immunol.* **180**, 8410–8420 (2008).
22. Xu, Y. *et al.* Toll-like receptor 4 is a sensor for autophagy associated with innate immunity. *Immunity* **27**, 135–144 (2007).
23. Delgado, M. A., Elmaoued, R. A., Davis, A. S., Kyei, G. & Deretic, V. Toll-like receptors control autophagy. *EMBO J.* **27**, 1110–1121 (2008).
24. Hara, T. *et al.* Suppression of basal autophagy in neural cells causes neurodegenerative disease in mice. *Nature* **441**, 885–889 (2006).
25. Komatsu, M. *et al.* Homeostatic levels of p62 control cytoplasmic inclusion body formation in autophagy-deficient mice. *Cell* **131**, 1149–1163 (2007).
26. Paludan, C. *et al.* Endogenous MHC class II processing of a viral nuclear antigen after autophagy. *Science* **307**, 593–596 (2005).
27. Maeda, S. *et al.* Nod2 mutation in Crohn's disease potentiates NF-κB activity and IL-1β processing. *Science* **307**, 737–738 (2005).
28. Ishikura, T. *et al.* Interleukin-18 overproduction exacerbates the development of colitis with markedly infiltrated macrophages in interleukin-18 transgenic mice. *J. Gastroenterol. Hepatol.* **18**, 960–969 (2003).
29. Izcue, A., Coombes, J. L. & Powrie, F. Regulatory T cells suppress systemic and mucosal immune activation to control intestinal inflammation. *Immunol. Rev.* **212**, 256–271 (2006).
30. Nakagawa, I. *et al.* Autophagy defends cells against invading group A Streptococcus. *Science* **306**, 1037–1040 (2004).

Supplementary Information is linked to the online version of the paper at www.nature.com/nature.

Acknowledgements We are grateful to T. Kitamura, S. Yamaoka and N. Mizushima for providing materials. We thank K. J. Ishii, M. Yamamoto and members of the Laboratory of Host Defense for discussions; Y. Fujiwara, M. Shiokawa, R. Nakayama and N. Kitagaki for technical assistance; and M. Hashimoto and E. Kamada for secretarial assistance. This work was in part supported by grants from NIH (AI070167) and the Ministry of Health, Labour and Welfare of Japan, and by Grant-in-Aid for Specially Promoted Research from the Ministry of Education, Culture, Sports, Science and Technology of Japan.

Author Contributions T.S. generated the Atg16L1-deficient mice and performed the immunological experiments. N.F. performed the cell biology experiments. N.Y. generated the retroviral vector. M.K. and K.T. generated the Atg7-deficient mice. T.T. performed histological analysis of mice. M.H.J., S.U., B.-G.Y., T.S., H.O., T.N., T.K. and O.T. helped with experiments. T.Y. designed the cell biology research. S.A. supervised the overall research project.

Author Information Reprints and permissions information is available at www.nature.com/reprints. Correspondence and requests for materials should be addressed to S.A. (akira@biken.osaka-u.ac.jp).

METHODS

Generation of Atg16L1-deficient mice. The fragment of the Atg16L1 gene was isolated from genomic DNA extracted from wild-type ES cells by PCR. A targeting vector was constructed by replacing exons 3, 4 and 5 of Atg16L1 with a neomycin-resistance gene cassette (neo), and a herpes simplex virus thymidine kinase driven by PGK promoter was inserted into the genomic fragment for negative selection. After the targeting vector was transfected into ES cells, G418 and gancyclovir doubly resistant colonies were selected and screened by PCR and Southern blotting. Homologous recombinants were micro-injected into C57BL/6 female mice, and heterozygous F1 progenies were intercrossed in order to obtain Atg16L1-deficient (Δ/Δ) mice. The Atg16L1-deficient mice used were on a 129Sv × C57BL/6 background.

For the generation of fetal liver chimaeric mice, fetal liver cells were harvested at E15.5 and injected into lethally irradiated CD45.1 or C57BL6J mice. Chimaeric mice were given antibiotics in drinking water for 2 months. The mice were analysed at least 3 months after reconstitution.

Mice were maintained in our animal facility and treated in accordance with the guidelines of Osaka University.

Reagents, mice and cells. Anti-IL-1β antibodies, recombinant mouse IFN-γ, ELISA kits for mouse IL-1β, human IL-1β, mouse IL-6 and mouse TNFα, were purchased from R&D Systems. Recombinant mouse IFN-β and the ELISA kit for mouse IFN-β were purchased from PBL InterferonSource. Anti-LC3 and anti-IL-18 antibodies and the ELISA kit for IL-18 were purchased from MBL International. GM-CSF and M-CSF were purchased from Peprotech. Anti-p62/SQSTM1 antibody was purchased from BIOMOL International. Anti-Atg12, anti-phospho-IRF3, anti-phospho-p38 and anti-phospho-ERK antibodies were purchased from Cell Signaling Technology. Anti-IκBα, anti-ERK and caspase-1 p10 were purchased from Santa Cruz Biotechnology. YVAD-fmk, wortmannin and FeTPPS were purchased from Calbiochem. ATP, oxidized ATP, LPS from *Salmonella minnesota* Re 595, 3-methyadenine, muramyl dipeptide and anti-α-tubulin antibody were purchased from Sigma. Lipid A was purchased from Peptide Institute. Flagellin was purchased from Invivogen. Uric acid crystals were purchased from Alexis. N-acetyl-L-cysteine was purchased from Nacalai Tesque. Poly(I)·poly(C) was purchased from GE Healthcare. R-848 was kindly provided by the Pharmaceuticals and Biotechnology Laboratory Japan Energy Corporation. CpG oligodeoxynucleotides (ODN1668) were synthesized at Hokkaido System Science Co. Anti-Atg16L1and anti-Atg5 antibodies were kindly donated by N. Mizushima (Tokyo Medical and Dental University).

K. pneumonia and *E. aerogenes* were kindly donated by the Research Institute of Microbial Disease, Osaka University. *E. coli* (DH5α) was purchased from TOYOBO. *Salmonella enteritica serovar typhimurium* (SR-11 × 3181) was provided by the Kitasato Institute for Life Science. Mice deficient in MyD88, TRIF or Atg7 were described previously[8,13]. Atg5-deficient MEFs and Plat-E cells were kindly donated by N. Mizushima and T. Kitamura (University of Tokyo), respectively. RAW264.7 cells were purchased from ATCC.

Plasmids. The retroviral expression constructs pMRX-ires-puro, pMRX-ires-bsr and pMRX-ires-EGFP (donated by S. Yamaoka) were derivatives of pMX (donated by T. Kitamura). Complementary DNA encoding human IL-1β was inserted into pMRX-ires-EGFP, generating pMRX-ires-IL-1β. Complementary DNA encoding Atg16L1 lacking in coiled-coil domain (Atg16L1 ΔCCDβ) was inserted into pMRX-ires-puro, generating pMRX-Atg16L1 ΔCCDβ-ires-puro. Complementary DNA encoding the GFP-Atg5 chimaeric protein was inserted into pMRX-ires-bsr, generating pMRX-GFP-Atg5-ires-bsr. Construction and inhibitory function details of pStrawberry-Atg4^{C74A} are described elsewhere[31].

RT–PCR. Total RNA was isolated using RNAeasy Mini kits (Qiagen) according to the manufacturer's instructions. Reverse transcription was performed using ReverTra Ace (TOYOBO) according to the manufacturer's instructions. For quantitative PCR, cDNA fragments were amplified by RealTime PCR Master Mix (TOYOBO) according to the manufacturer's instructions. Fluorescence from the Taqman probe for each cytokine was detected by a 7500 Real-Time PCR System (Applied Biosystems). To determine the relative induction of cytokine mRNA in response to LPS stimulation, the mRNA expression level of each cytokine was normalized to the expression level of 18S RNA. The experiments were repeated at least twice. The results were reproducible.

The primer pairs used in Supplementary Fig. 1 are as follows. Primer pair A (exon 1-2), 5′-GTTCGGCATGTCGTCGGGCCTG-3′ and 5′-ATTTCATGCC-TATTTGGCATGTCATGC-3′. Primer pair B (exon 6-7), 5′-GTCAAGCACG-GCTGCAGAAGGAGCTTG-3′ and 5′-GTAGCTGCTCTGCTGACAGCTCGG-3′. Primer pair C (exon 1-5), 5′-GTTCGGCATGTCGTCGGGCCTGN-3′ and 5′-GACCAGTTCCTGGTTCTCCTCAGTAG-3′. Primer pair D (exon 5-7), 5′-CGCCTCAATGCAGAGAATGAGAAGGAC-3′ and 5′-GTAGCTGCTCTGCT-GACAGCTCGG-3′. Primer pair E (exon 1-6), 5′-GTTCGGCATGTCGTCG-GGCCTG-3′ and 5′-CAAGCTCCTTCTGCAGCCGTGCTTGAC-3′.

Bulk protein degradation assay. Cells were exchanged into labelling medium containing ^{14}C-valine (1.5 μCi ml^{-1}) and incubated overnight. Cells were exchanged into chase medium (DMEM supplemented with 10% FBS and 10 mM unlabelled valine) and further incubated for 4 h to remove the contribution of short-lived proteins. After the chase period, cells were exchanged into HBSS containing 10 mM valine to induce autophagy. After a 2 h incubation, the media were collected and the trichloroacetic acid (TCA)-soluble fraction was analysed by scintillation counting. Cells were lysed in ice-cold RIPA buffer and the TCA-insoluble fraction was isolated and analysed by scintillation counting. To determine the rate of long-lived protein degradation, the count in the TCA-soluble fraction in the medium was divided by the equivalent TCA-insoluble count in the cell.

Detection of apoptosis. The appearance of mono/oligo-nucleosomes, markers for apoptosis, was detected by Cell Death Detection ELISA^{PLUS} (Roche). Chromatin condensation in apoptotic nuclei was detected using an ApoStrand ELISA Apoptosis Detection Kit (Biomol). The experiments were repeated twice, and the results were reproducible.

Determination of bacteria colony forming units (c.f.u.s). Levels of c.f.u.s in freshly isolated faeces or spleen were determined by homogenization of material in PBS/0.01% Triton X-100 followed by serial dilution plating on non-selective Luria-Bertani agar.

31. Fujita, N. *et al.* An Atg4B mutant hampers the lipidation of LC3 paralogues and causes defects in autophagosome closure. *Mol. Biol. Cell* advance online publication, doi:10.1091/mbc.E08-03-0312 (3 September 2008).

nature immunology

Sequential control of Toll-like receptor–dependent responses by IRAK1 and IRAK2

Tatsukata Kawagoe[1,2], Shintaro Sato[3], Kazufumi Matsushita[1,2], Hiroki Kato[1,2], Kosuke Matsui[2], Yutaro Kumagai[1,2], Tatsuya Saitoh[1,2], Taro Kawai[1–3], Osamu Takeuchi[1–3] & Shizuo Akira[1–3]

Members of the IRAK family of kinases mediate Toll-like receptor (TLR) signaling. Here we show that IRAK2 was essential for sustaining TLR-induced expression of genes encoding cytokines and activation of the transcription factor NF-κB, despite the fact that IRAK2 was dispensable for activation of the initial signaling cascades. IRAK2 was activated 'downstream' of IRAK4, like IRAK1, and TLR-induced cytokine production was abrogated in the absence of both IRAK1 and IRAK2. Whereas the kinase activity of IRAK1 decreased within 1 h of TLR2 stimulation, coincident with IRAK1 degradation, the kinase activity of IRAK2 was sustained and peaked at 8 h after stimulation. Thus, IRAK2 is critical in late-phase TLR responses, and IRAK1 and IRAK2 are essential for the initial responses to TLR stimulation.

Toll-like receptors (TLRs) sense the invasion of microbes in the body by recognizing their structural components and activate intracellular signaling pathways leading to the expression of genes responsible for inflammatory and immune responses[1–3]. Studies have identified specific components detected by each TLR, such as diacyl lipoprotein (TLR6 and TLR2), triacyl lipoprotein (TLR1 and TLR2), double-stranded RNA (TLR3), lipopolysaccharide (LPS; TLR4), flagellin (TLR5), single-stranded RNA (TLR7 and TLR8) and CpG DNA (TLR9). Stimulation with TLR ligands induces the formation of homo- or heterodimers of TLRs for the recruitment of adaptor molecules containing the Toll–interleukin 1 receptor (IL-1R) homology domain (TIR domain). MyD88, an adaptor containing a TIR domain and a death domain, is essential for signaling 'downstream' of various TLRs, except TLR3 (refs. 4,5). MyD88 interacts with members of the IL-1R-associated kinase (IRAK) family, which dissociate from MyD88 and interact with tumor necrosis factor (TNF) receptor–associated factor 6 (TRAF6). TRAF6 acts as an ubiquitin protein ligase to catalyze the formation of a Lys63-linked polyubiquitin chain on TRAF6 itself and on the transcription factor NF-κB modulator NEMO. Transforming growth factor-β–activated kinase 1 (TAK1) is also recruited to TRAF6 and then phosphorylates inhibitor of NF-κB (IκB) kinase-β (IKKβ) and mitogen-activated protein (MAP) kinase kinase 6. Subsequently, the IKK complex, composed of IKKα, IKKβ and NEMO, is formed. NF-κB binds to IκB in resting cells, where it is sequestered in the cytoplasm. Phosphorylation of IκB by the IKK complex leads to degradation of IκB by the ubiquitin-proteasome system, freeing NF-κB to translocate into the nucleus, where it activates the expression of genes encoding proinflammatory cytokines. Activation of the MAP kinase cascade is responsible for gene expression induced by the transcription activator AP-1.

There are three additional TIR domain–containing adaptors involved in TLR signaling. TIRAP (also called Mal) has been shown to be critical for TLR2- and TLR4-induced NF-κB activation[6–9]. TLR3 and TLR4 trigger the signaling cascade leading to the production of type I interferons through another adaptor, TRIF[10–12]. The fourth adaptor, TRAM, bridges TLR4 and TRIF[13] and is critical for TLR4-induced interferon-inducible gene expression[14,15].

The IRAK family has four members: IRAK1 (A001277), IRAK2 (A001278), IRAKM and IRAK4 (A003450)[16]. IRAK family members are composed of an amino-terminal death domain and a serine-threonine kinase domain. IRAK4 is known to be essential for TLR–IL-1R-mediated cellular responses[17–19]. The kinase activity of IRAK4 is essential for its function in TLR-induced cytokine production[20–22]. IRAK4 deficiency in humans also leads to impaired TLR responses together with recurrent infections with pyrogenic bacteria, particularly *Streptococcus pneumoniae*[23–26]. In contrast, cells lacking IRAKM showed increased cytokine production in response to TLR stimuli, and IRAKM functions to inhibit formation of the IRAK1-TRAF6 complex[27]. IRAK1, the first member of the IRAK family to be discovered, is also involved in TLR–IL-1R signaling pathways[28]. IRAK1-deficient mice are more resistant to LPS-induced shock than are wild-type control mice[29,30], although *Irak4*$^{-/-}$ mice and *Myd88*$^{-/-}$ mice are more resistant to LPS inoculation[5,17,22]. IRAK1-deficient fibroblasts and macrophages reportedly show impaired cytokine production in response to IL-1β or LPS[4,17]. However, IRAK1-deficient cells are still able to produce cytokines after TLR or IL-1R stimulation, and it has been hypothesized that other IRAK family members or

[1]Laboratory of Host Defense, World Premier International Research Center, Immunology Frontier Research Center [2]Research Institute for Microbial Diseases, Osaka University, [3]Exploratory Research for Advanced Technology, Japan Science and Technology Agency, 3-1 Yamada-oka, Suita, Osaka 565-0871, Japan. Correspondence should be addressed to S.A. (sakira@biken.osaka-u.ac.jp).

Received 20 December 2007; accepted 10 March 2008; published online 27 April 2008; doi:10.1038/ni.1606

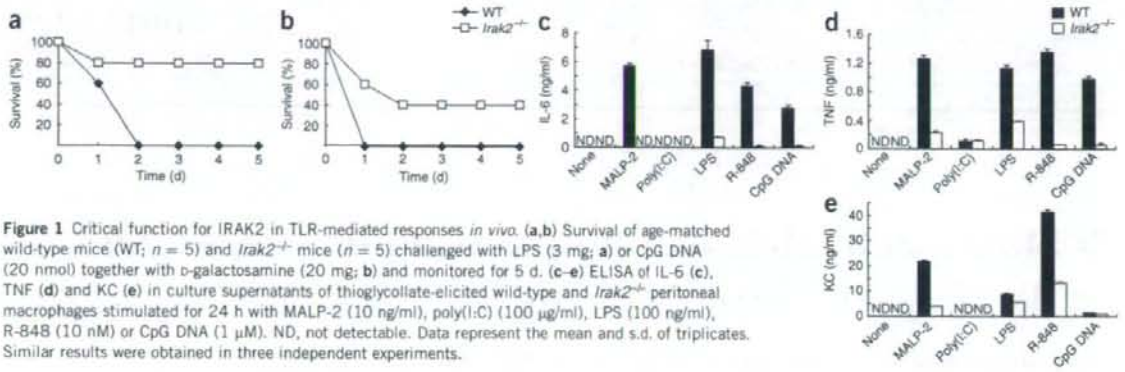

Figure 1 Critical function for IRAK2 in TLR-mediated responses *in vivo*. (**a**,**b**) Survival of age-matched wild-type mice (WT; $n = 5$) and *Irak2*$^{-/-}$ mice ($n = 5$) challenged with LPS (3 mg; **a**) or CpG DNA (20 nmol) together with D-galactosamine (20 mg; **b**) and monitored for 5 d. (**c**–**e**) ELISA of IL-6 (**c**), TNF (**d**) and KC (**e**) in culture supernatants of thioglycollate-elicited wild-type and *Irak2*$^{-/-}$ peritoneal macrophages stimulated for 24 h with MALP-2 (10 ng/ml), poly(I:C) (100 μg/ml), LPS (100 ng/ml), R-848 (10 nM) or CpG DNA (1 μM). ND, not detectable. Data represent the mean and s.d. of triplicates. Similar results were obtained in three independent experiments.

other proteins could take over the function of IRAK1. Instead, given that IRAK1 is critical for the actions of TLR9-mediated type I interferons but not for the actions of proinflammatory cytokines in plasmacytoid dendritic cells, it is most likely that the main contribution of IRAK1 to the TLR responses of plasmacytoid dendritic cells is in the regulation of interferon-regulatory factors but not of NF-κB[31].

IRAK2 is suggested to be involved in signaling through TIRAP, the adaptor protein responsible for TLR2 and TLR4 responses[6]. Overexpression of IRAK2 in cells results in NF-κB activation[32,33]. IRAK2 is also involved in TLR3 and TLR8 signaling[34]. However, the function of IRAK2 *in vivo* and its relation to other IRAK family members are not yet understood. It has remained unclear whether IRAK2 functions as an active kinase, as a critical aspartate residue in the IRAK catalytic domain is an asparagine residue in IRAK2, and IRAK2 fails to undergo autophosphorylation, unlike IRAK1 and IRAK4 (ref. 35).

Here we generated *Irak2*$^{-/-}$ mice and investigated the function of IRAK2 in TLR responses. *Irak2*$^{-/-}$ mice were resistant to TLR4- and TLR9-mediated shock responses and *Irak2*$^{-/-}$ cells showed impaired production of proinflammatory cytokines. IRAK2 was essential for sustaining TLR-mediated expression of genes encoding proinflammatory cytokines. Recruitment of NF-κB to the *Il6* promoter within 8 h of TLR2 stimulation was impaired in *Irak2*$^{-/-}$ macrophages, which suggested that IRAK2 is critical for sustaining IL-6 promoter activation. Macrophages lacking both IRAK1 and IRAK2 showed substantial defects in the induction of genes encoding proinflammatory cytokines in response to TLR ligands relative to that of cells lacking either IRAK alone, which indicated that IRAK1 and IRAK2 function redundantly in the TLR signaling pathway. An intact kinase domain of IRAK2 was essential for TLR-induced cytokine production, and the kinase activity of IRAK2 was sustained for longer than that of IRAK1 after TLR stimulation. Our results indicate that IRAK2 is critical in late-phase TLR responses and that IRAK1 and IRAK2 function redundantly in the initial response.

RESULTS

Essential function for IRAK2 in TLR-induced responses

To investigate the function of IRAK2 *in vivo*, we generated *Irak2*$^{-/-}$ mice by homologous recombination of embryonic stem cells. We targeted exons 4, 5 and 6 of mouse *Irak2* with a neomycin-resistance cassette in embryonic stem cells and established *Irak2*$^{-/-}$ mice (**Supplementary Fig. 1a** online). We confirmed homologous recombination of the *Irak2* locus by Southern blot analysis (**Supplementary Fig. 1b**). Expression of IRAK2 mRNA and protein was abrogated in *Irak2*$^{-/-}$ cells (**Supplementary Fig. 1c,d**). *Irak2*$^{-/-}$ mice grew normally and did not show any gross abnormalities until the age of 24 weeks. Flow cytometry showed that the spleens and lymph nodes of wild-type and *Irak2*$^{-/-}$ mice did not have a different composition of T cells, B cells, macrophages and dendritic cells (data not shown).

We first examined the function of IRAK2 in response to stimulation with TLR ligands *in vivo*. After challenge with LPS or CpG DNA together with D-galactosamine, all wild-type mice succumbed to shock and died. In contrast, *Irak2*$^{-/-}$ mice were more resistant to such challenge; 80% and 40% of mice survived after challenge with LPS and CpG DNA, respectively (**Fig. 1a,b**). These results indicate that IRAK2 is critical for TLR-induced shock *in vivo*. We next examined cytokine production by macrophages in response to TLR ligands, including MALP-2 (TLR6-TLR2), polyinosinic-polycytidylic acid (poly(I:C); TLR3), LPS (TLR4), resiquimod (R-848; TLR7) and CpG DNA (TLR9). We stimulated thioglycollate-elicited peritoneal macrophages with each TLR ligand and measured the production of proinflammatory cytokines by enzyme-linked immunoassay (ELISA). The production of IL-6, TNF and the inflammatory chemokine KC in response to these TLR ligands, except poly(I:C), was considerably impaired in *Irak2*$^{-/-}$ macrophages relative to that in wild-type cells (**Fig. 1c–e**). In contrast, TNF production in response to poly(I:C) was not different for wild-type versus *Irak2*$^{-/-}$ macrophages. Conventional dendritic cells from *Irak2*$^{-/-}$ mice also showed defective cytokine production in response to these TLR ligands (data not shown). Thus, IRAK2 is

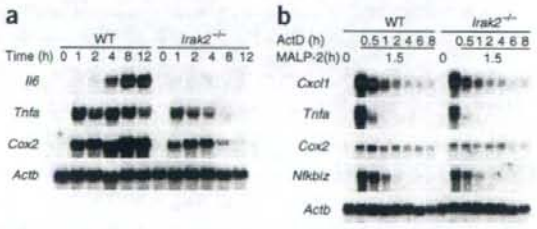

Figure 2 Impaired MALP-2-induced gene expression in *Irak2*$^{-/-}$ cells. (**a**) RNA blot analysis of the expression of *Il6*, *Tnfa* and *Cox2* in wild-type and *Irak2*$^{-/-}$ peritoneal macrophages stimulated for various times (above lanes) with MALP-2 (10 ng/ml). Bottom, rehybridization of same membrane with an *Actb* probe. (**b**) RNA blot analysis of the expression of *Cxcl1*, *Tnfa* and *Nfkbiz* in peritoneal macrophages left untreated (0) or treated for 1.5 h with MALP-2 (10 ng/ml) and then treated for various times (above lanes; ActD) with actinomycin D (5 μg/ml) and MALP-2 (10 ng/ml). Bottom, rehybridization of same membrane with an *Actb* probe. Similar results were obtained in three independent experiments.

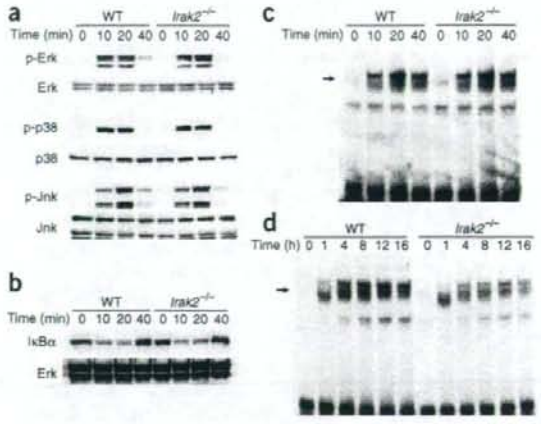

Figure 3 Activation of NF-κB and MAP kinases in *Irak2*$^{-/-}$ macrophages in response to MALP-2. (**a**,**b**) Immunoblot of whole-cell lysates of wild-type and *Irak2*$^{-/-}$ peritoneal macrophages stimulated for various times (above lanes) with MALP-2, analyzed with antibody to phosphorylated (p-) Erk, p38 or Jnk (**a**) or anti-IκBα (**b**). Total Erk, p38 and Jnk serve as a loading control. (**c**,**d**) EMSA of NF-κB DNA-binding activity in nuclear extracts of wild-type and *Irak2*$^{-/-}$ macrophages stimulated for various times (above lanes) with MALP-2 (10 ng/ml), assessed with an NF-κB-specific probe. Arrows indicate the induced NF-κB complex. Results are representative of three independent experiments.

important for eliciting cytokine production in response to various TLR ligands, except for a TLR3 ligand.

TLR-mediated gene expression in *Irak2*$^{-/-}$ macrophages

We next determined by RNA blot analysis whether the impaired cytokine production resulting from IRAK2 deficiency occurred at the 'message' level. We chose MALP-2, a TLR2 ligand, as the stimulant, because TLR2 signals only through the MyD88-dependent pathway. In response to stimulation with MALP-2, wild-type macrophages expressed *Il6*, *Tnf* (called '*Tnfa*' here) and *Ptgs2* (called '*Cox2*' here; **Fig. 2a**). In contrast, *Irak2*$^{-/-}$ macrophages failed to express *Il6* in response to stimulation with MALP-2. However, expression of *Tnfa* and *Cox2* was induced normally at 1 h after stimulation, even in the absence of IRAK2, and then was attenuated at 4 h after stimulation. Thus, we hypothesized that IRAK2 signaling was involved in regulating the mRNA stability of TLR-inducible genes. To examine the possible regulation of mRNA stability by IRAK2, we stimulated peritoneal macrophages from wild-type and *Irak2*$^{-/-}$ mice with MALP-2 for 1.5 h, then treated them with actinomycin D for an additional 0.5–8 h (**Fig. 2b**). The abundance of mRNA of TLR-inducible genes such as *Cxcl1*, *Tnfa*, *Cox2* and *Nfkbiz* gradually decreased after actinomycin D treatment with a similar time course in wild-type and *Irak2*$^{-/-}$ macrophages, which indicated that the impaired cytokine gene expression in *Irak2*$^{-/-}$ cells was not due to mRNA instability.

Next we examined the activation of signaling molecules, including MAP kinases and NF-κB, in *Irak2*$^{-/-}$ macrophages. Activation of the MAP kinases Jnk, p38 and Erk by MALP-2 was not impaired in *Irak2*$^{-/-}$ macrophages (**Fig. 3a**), which indicated that IRAK2 is dispensable for TLR-induced MAP kinase activation. We then analyzed NF-κB activation. In response to stimulation with MALP-2, IκBα was degraded within 10 min (**Fig. 3b**) and NF-κB DNA-binding activity was induced (**Fig. 3c**) in wild-type macrophages. It is well known that NF-κB induces the expression of IκB proteins, leading to the restoration of IκBα protein abundance to that seen before stimulation within 40 min. The degradation and recovery of IκBα protein, as well as NF-κB DNA-binding activity, were not impaired in *Irak2*$^{-/-}$ macrophages. Next we examined whether IRAK2 controls NF-κB activation later after stimulation with MALP-2. NF-κB DNA-binding activity was sustained until 16 h after stimulation in wild-type macrophages (**Fig. 3d**). In contrast, activation beyond 4 h after stimulation was impaired in *Irak2*$^{-/-}$ cells. Gel mobility 'supershift' assays showed that the p65 and p50 subunits of NF-κB were activated in both wild-type and *Irak2*$^{-/-}$ cells (**Supplementary Fig. 2** online). Antibodies to other NF-κB subunits such as c-Rel and p52 failed to produce 'supershifting' of NF-κB in wild-type or *Irak2*$^{-/-}$ macrophages, which suggested that the composition of NF-κB was not altered in wild-type versus *Irak2*$^{-/-}$ cells. These results indicate that IRAK2 is critical for sustaining NF-κB activation after TLR stimulation.

Requirement for IRAK2 kinase activity in the TLR signaling

It has been reported that IRAK2 overexpressed in IRAK1-deficient human embryonic kidney 293 (I1A) cells is unable to

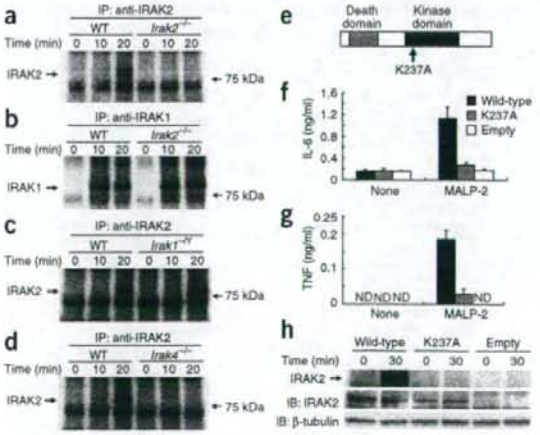

Figure 4 Requirement for IRAK2 kinase activity in the response to stimulation with MALP-2. (**a**–**d**) *In vitro* kinase assay of the activation of IRAK1 and IRAK2 in wild-type and *Irak2*$^{-/-}$ (**a**,**b**), *Irak1*$^{-/Y}$ (**c**) or *Irak4*$^{-/-}$ (**d**) peritoneal macrophages stimulated for various times (above lanes) with MALP-2 (10 ng/ml); cell lysates were immunoprecipitated (IP) with anti-IRAK2 (**a**,**c**,**d**) or anti-IRAK1 (**b**). kDa, kilodaltons. Data are representative of three independent experiments. (**e**–**h**) Requirement for IRAK2's kinase activity in the response to TLR stimulation. (**e**) Mutant IRAK2 construct, containing a point substitution of the lysine at position 237 with an alanine residue (K237A). (**f**,**g**) ELISA of IL-6 (**f**) and TNF (**g**) in culture supernatants of macrophages generated from *Irak2*$^{-/-}$ bone marrow cells retrovirally transduced with wild-type or K237A IRAK2; macrophages were stimulated for 24 h with MALP-2 (10 ng/ml). Data represent the mean and s.d.; similar results were obtained in three independent experiments. (**h**) *In vitro* kinase assay of the kinase activity of IRAK2 (top) and immunoblot (IB) analysis of IRAK2 expression (middle) in retrovirally transduced bone marrow cells stimulated for 30 min with MALP-2 (10 ng/ml); lysates were immunoprecipitated with anti-IRAK2 for the kinase assay. Bottom, immunoblot analysis of β-tubulin (loading control). Data are representative of three independent experiments.

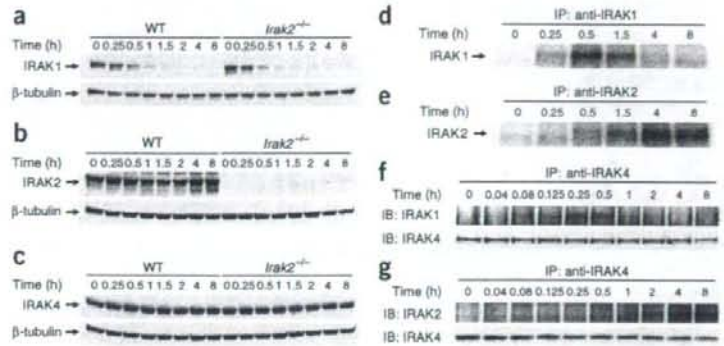

Figure 5 Sequential activation of IRAK1 and IRAK2 kinase activity after stimulation with MALP-2. (**a–c**) Immunoblot analysis of the expression of IRAK1 (**a**), IRAK2 (**b**) and IRAK4 (**c**) in response to stimulation with MALP-2. Bottom, immunoblot analysis of β-tubulin (loading control). Similar results were obtained in two independent experiments. (**d,e**) *In vitro* kinase assay of the activation of IRAK1 and IRAK2 in peritoneal macrophages stimulated for various times (above lanes) with MALP-2 (10 ng/ml); lysates were immunoprecipitated with anti-IRAK1 (**d**) or anti-IRAK2 (**e**). Data are representative of three independent experiments. (**f,g**) Immunoassay of wild-type macrophages stimulated for various times (above lanes) with MALP-2 (10 ng/ml); lysates were immunoprecipitated with anti-IRAK4, followed by immunoblot analysis with anti-IRAK1 (**f**) or anti-IRAK2 (**g**). Below, immunoblot analyses of IRAK4 serve as a loading control. Similar results were obtained in three independent experiments.

autophosphorylate because of the substitution in its kinase domain[35]. Nevertheless, all IRAK family members contain a functional ATP-binding pocket with an invariant lysine residue in the protein kinase subdomain[16]. Expression of IRAK1 and IRAK2 together leads to phosphorylation of IRAK2, whereas the expression of IRAK2 with a substitution (KK237AA) in its ATP-binding pocket fails to induce IRAK2 phosphorylation, which suggests that IRAK2 may function as an active kinase when phosphorylated by IRAK1 (ref. 35). To determine whether IRAK2 has intrinsic kinase activity in response to TLR stimulation *in vivo*, we immunoprecipitated IRAK2 from MALP-2-stimulated macrophages and did an *in vitro* kinase assay. IRAK2 phosphorylation was induced after 20 min in wild-type but not *Irak2*$^{-/-}$ macrophages in response to TLR2 stimulation (**Fig. 4a**). In contrast, IRAK2 deficiency did not affect MALP-2-induced IRAK1 autophosphorylation (**Fig. 4b**). The extent of IRAK2 phosphorylation was not different in wild-type versus IRAK1-deficient (*Irak1*$^{-/Y}$) macrophages (**Fig. 4c**), which indicated that IRAK2 was not phosphorylated by coprecipitated IRAK1. Furthermore, *Irak4*$^{-/-}$ macrophages failed to induce IRAK2 phosphorylation (**Fig. 4d**), which indicated that IRAK4 is essential for the activation of IRAK2.

We next determined whether IRAK2 kinase activity is required for its function. We retrovirally expressed wild-type IRAK2 or a kinase-defective IRAK2 mutant with a K237A substitution (**Fig. 4e**) in *Irak2*$^{-/-}$ macrophages and assessed the responses of the cells to TLR stimulation. The populations of CD11b^{+} cells expressing retroviral constructs were similar for cells transduced with wild-type or K237A IRAK2 (**Supplementary Fig. 3a** online). Immunoblot analysis confirmed the expression of both wild-type and K237A IRAK2 (**Supplementary Fig. 3b**). Reconstitution of *Irak2*$^{-/-}$ macrophages with wild-type IRAK2 increased the production of IL-6 and TNF in response to stimulation with MALP-2. In contrast, K237A IRAK2 failed to restore MALP-2 responsiveness (**Fig. 4f,g**). Furthermore, reconstitution with wild-type IRAK2 restored the phosphorylation of IRAK2 in response to stimulation with MALP-2, but reconstitution with K237A IRAK2 did not (**Fig. 4h**), which confirmed that an intact kinase domain is essential for IRAK2 phosphorylation. These results indicate that IRAK2 kinase activity is indispensable for its function *in vivo*.

Sustained activation of IRAK2 after TLR2 stimulation

IRAK1 is known to be ubiquitinated and degraded after IL-1β stimulation[36,37]. However, it remains unknown how expression of IRAK2 and IRAK4 is regulated in response to TLR stimulation. In response to stimulation with MALP-2, there was a decrease in IRAK1 protein within 30 min of stimulation, and it remained suppressed for up to 8 h after stimulation (**Fig. 5a**). We noted a similar decrease in IRAK1 expression in *Irak2*$^{-/-}$ macrophages. In contrast, the abundance of IRAK2 or IRAK4 protein was not altered in response to stimulation with MALP-2 (**Fig. 5b,c**). The activation of IRAK1 autophosphorylation was induced rapidly and peaked at 0.5 h after stimulation with MALP-2 (**Fig. 5d**). Subsequently, this autophosphorylation decreased coincidentally with the diminished expression of IRAK1 protein. Notably, MALP-2-induced IRAK2 phosphorylation was sustained up to 8 h after stimulation (**Fig. 5e**). We further

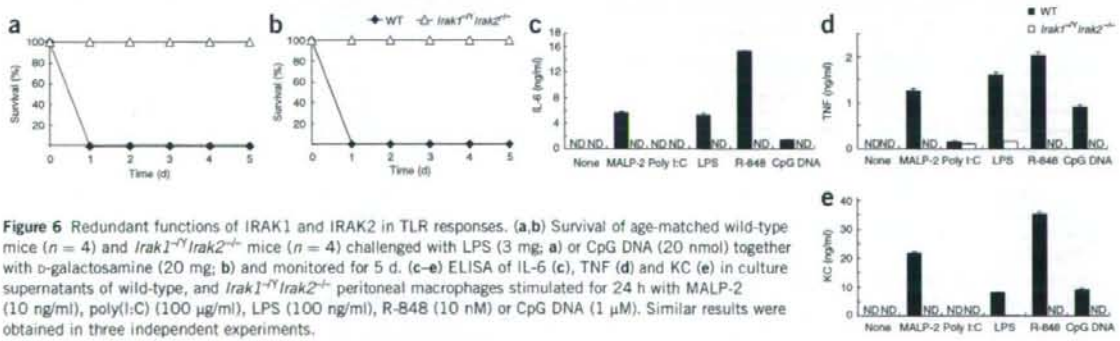

Figure 6 Redundant functions of IRAK1 and IRAK2 in TLR responses. (**a,b**) Survival of age-matched wild-type mice ($n = 4$) and *Irak1*$^{-/Y}$*Irak2*$^{-/-}$ mice ($n = 4$) challenged with LPS (3 mg; **a**) or CpG DNA (20 nmol) together with D-galactosamine (20 mg; **b**) and monitored for 5 d. (**c–e**) ELISA of IL-6 (**c**), TNF (**d**) and KC (**e**) in culture supernatants of wild-type, and *Irak1*$^{-/Y}$*Irak2*$^{-/-}$ peritoneal macrophages stimulated for 24 h with MALP-2 (10 ng/ml), poly(I:C) (100 μg/ml), LPS (100 ng/ml), R-848 (10 nM) or CpG DNA (1 μM). Similar results were obtained in three independent experiments.

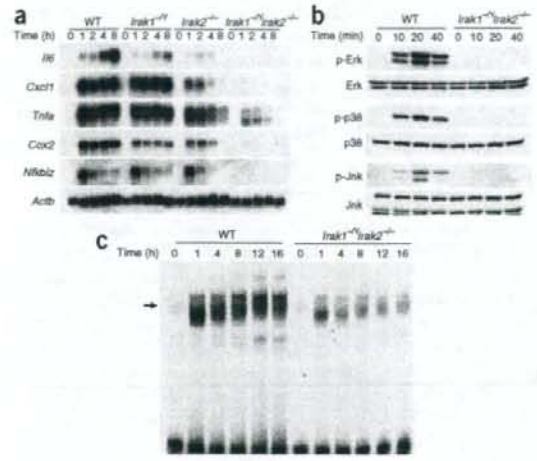

Figure 7 Double deficiency in IRAK1 and IRAK2 causes impaired signaling and is similar to IRAK4 deficiency. (**a**) RNA blot analysis of the expression of *Il6*, *Cxcl1*, *Tnfa*, *Cox2* and *Nfkbiz* in peritoneal macrophages stimulated for various times (above lanes) with MALP-2 (10 ng/ml). Bottom, rehybridization of same membrane with an *Actb* probe. (**b**) Immunoblot analysis of phosphorylated Erk, p38 and Jnk in whole-cell lysates of wild-type and *Irak1*$^{-/Y}$*Irak2*$^{-/-}$ macrophages stimulated with MALP-2. Total Erk, p38 and Jnk serve as a loading control. (**c**) EMSA of nuclear extracts of MALP-2-stimulated wild-type and *Irak1*$^{-/Y}$*Irak2*$^{-/-}$ macrophages, analyzed with an NF-κB-specific probe. Arrow indicates the induced NF-κB complex. Data are representative of three independent experiments.

examined association between IRAK4 and IRAK1 or IRAK2 in response to stimulation with MALP-2. The association between IRAK4 and IRAK1 was induced 5 min after stimulation and decreased at 1 h after stimulation (**Fig. 5f**). In contrast, IRAK2 was precipitated together with IRAK4 at later time points and this was sustained until 8 h after stimulation (**Fig. 5g**). These results suggest that IRAK1 and IRAK2 are activated in response to TLR stimulation at early and late time points, respectively.

Relationship between IRAK1 and IRAK2 in TLR responses

The differential activation of IRAK1 and IRAK2 suggested that these kinases function redundantly in TLR signaling and responses. The production of TNF, IL-6 and KC in response to TLR ligands was modestly impaired in *Irak1*$^{-/Y}$ macrophages (**Supplementary Fig. 4** online). Therefore, we generated mice doubly deficient in IRAK1 and IRAK2 (*Irak1*$^{-/Y}$*Irak2*$^{-/-}$ mice) and examined their responses to TLR simulation. When we inoculated wild-type and *Irak1*$^{-/Y}$*Irak2*$^{-/-}$ mice with LPS or CpG DNA, *Irak1*$^{-/Y}$*Irak2*$^{-/-}$ mice were completely resistant to septic shock induced by LPS or CpG DNA (**Fig. 6a,b**). The production of IL-6, TNF and KC in response to these TLR ligands, except poly(I:C), was abrogated in *Irak1*$^{-/Y}$*Irak2*$^{-/-}$ macrophages (**Fig. 6c–e**).

We next analyzed MALP-2-induced mRNA expression in peritoneal macrophages (**Fig. 7a**). In response to stimulation with MALP-2, *Irak1*$^{-/Y}$*Irak2*$^{-/-}$ macrophages failed to express *Il6*, *Cxcl1*, *Cox2* or *Nfkbiz*, even at early time points. Although *Tnfa* was expressed in response to MALP-2 even in the absence of IRAK1 and IRAK2, its expression was lower in *Irak1*$^{-/Y}$*Irak2*$^{-/-}$ macrophages. Analysis of signaling molecules showed that IRAK1 and IRAK2 were essential for the activation of MAP kinases, including Jnk, p38 and Erk (**Fig. 7b**). Nevertheless, NF-κB DNA-binding activity was induced after stimulation with MALP-2, even in *Irak1*$^{-/Y}$*Irak2*$^{-/-}$ macrophages, although the activity was lower (**Fig. 7c**).

IRAK1 and IRAK2 have been linked to the response to IL-1β. The production of IL-6 in response to IL-1β in *Irak2*$^{-/-}$ and *Irak1*$^{-/Y}$ mouse embryonic fibroblasts was impaired relative to that in wild-type mouse embryonic fibroblasts and was abrogated in *Irak1*$^{-/Y}$*Irak2*$^{-/-}$ mouse embryonic fibroblasts (**Supplementary Fig. 5** online), which indicated that IRAK1 and IRAK2 are involved in the IL-1R signaling.

These findings collectively suggest that IRAK1 and IRAK2 function redundantly in TLR and IL-1R signaling downstream of IRAK4. The defects in the MALP-2 responsiveness of *Irak1*$^{-/Y}$*Irak2*$^{-/-}$ macrophages are reminiscent of those of *Irak4*$^{-/-}$ macrophages[22]. Therefore, these results indicate that either IRAK1 or IRAK2 is required for IRAK4 signaling.

Gene expression in the absence of IRAK1 and IRAK2

Finally, we examined the expression of MALP-2-inducible genes in wild-type, *Irak2*$^{-/-}$ and *Irak1*$^{-/Y}$*Irak2*$^{-/-}$ macrophages by microarray analysis. In wild-type macrophages, in response to stimulation with MALP-2, 171 genes were upregulated more than tenfold at 2, 4 or 8 h after stimulation; we defined these as 'MALP-2-inducible genes' (**Supplementary Table 1** online). As shown by a 'heat map' of MALP-2-inducible genes in wild-type, *Irak2*$^{-/-}$ and *Irak1*$^{-/Y}$*Irak2*$^{-/-}$ macrophages, the expression of various MALP-2-inducible genes at 2 h after stimulation was similar in wild-type and *Irak2*$^{-/-}$ macrophages (**Fig. 8**). Nevertheless, the expression of most genes in *Irak2*$^{-/-}$ cells was lower by 8 h after stimulation. This finding is consistent with impaired activation of NF-κB at later time points. In the absence of both IRAK1 and IRAK2, the expression of MALP-2-inducible genes was impaired much more substantially. However, their expression was not completely abrogated, which suggests that signaling pathways independent of the IRAK family are involved in the regulation of TLR2-inducible genes.

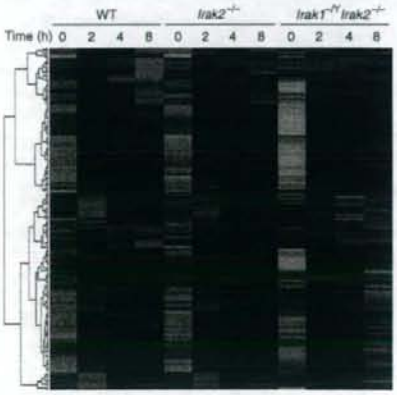

Figure 8 Expression of MALP-2-inducible genes in IRAK1- and IRAK2-deficient macrophages. Cluster images of microarray analysis (heat map and dendrogram) of MALP-2-inducible genes in wild-type, *Irak2*$^{-/-}$ and *Irak1*$^{-/Y}$*Irak2*$^{-/-}$ macrophages stimulated for various times (above columns) with MALP-2 (10 ng/ml). Genes upregulated more than tenfold in wild-type macrophages at 2, 4 or 8 h after stimulation were defined as 'MALP-2-inducible genes'.

DISCUSSION

In this study we generated *Irak2*$^{-/-}$ mice and examined the function of IRAK2 in TLR signaling, relative to that of IRAK1. *Irak2*$^{-/-}$ mice were resistant to shock responses mediated by LPS and CpG DNA. Although *Irak1*$^{-/Y}$ mice are also reported to be resistant to LPS shock, the difference in the mortality rates of wild-type and *Irak1*$^{-/Y}$ mice is subtle[38]. Thus, IRAK2 seems to be more involved in the mortality caused by TLR stimulation *in vivo* than is IRAK1. IRAK2 deficiency attenuated responses to various TLR ligands, including MALP-2, LPS, R-848 and CpG DNA, with the lone exception of poly(I:C). IL-1β-induced cytokine production was also impaired in *Irak2*$^{-/-}$ cells. Although previous results have suggested that IRAK2 acts downstream of TIRAP, an adaptor responsible for TLR2 and TLR4 signaling, our findings here have indicated that IRAK2 is critical not only for the TLR2 and TLR4 signaling pathways but also for the signaling pathways downstream of other TLRs with MyD88.

IRAK2 is critical for sustaining the expression of genes encoding proinflammatory cytokines in response to TLR stimulation. Although the initial upregulation of *Tnfa* and *Cxcl1* in response to TLR2 stimulation was not different control versus *Irak2*$^{-/-}$ macrophages, their expression was lower in *Irak2*$^{-/-}$ macrophages 4 h after stimulation. Thus, the amount of TNF protein produced during the initial 24 h was much lower in *Irak2*$^{-/-}$ macrophages. Although we hypothesized that IRAK2 was essential for ensuring the stability of mRNA encoding various cytokines, there was no difference in the degradation of cytokine transcripts in wild-type versus *Irak2*$^{-/-}$ macrophages. Thus, it seems that IRAK2 is important for sustaining the transcription of genes encoding proinflammatory cytokines involved in TLR signaling. Indeed, NF-κB DNA-binding activity was lower at later time points after TLR2 stimulation, which indicated that IRAK2-dependent signaling is critical for sustaining the activation of transcription factors such as NF-κB.

It has been reported that IRAK2 is involved in the activation of a MyD88-independent signaling pathway by activating TIRAP[6]. Another report has shown that IRAK2 is involved in TLR3 signaling 'upstream' of TRIF[34]. However, we found that TLR4-induced interferon-inducible gene expression was not impaired in *Irak2*$^{-/-}$ macrophages (data not shown). In addition, cytokine production in response to poly(I:C) stimulation was not impaired in *Irak2*$^{-/-}$ or *Irak1*$^{-/Y}$*Irak2*$^{-/-}$ macrophages. Although the reason for discrepancy with previous reports is not clear, we believe that IRAK2 is involved in MyD88-dependent signaling pathways but not in the TRIF-dependent pathway emanating from TLR4.

Among IRAK family members, IRAK1 and IRAK4 have been shown to have intrinsic kinase activity[39,40]. However, a critical aspartate residue in the IRAK catalytic domain is an asparagine or serine in IRAK2 or IRAKM, and their kinase domains are supposedly inactive. However, it has also been shown that coexpression of IRAK1 and IRAK2 leads to phosphorylation of IRAK2, whereas expression of IRAK2 with a substitution in its ATP-binding pocket (KK237AA) together with IRAK1 fails to induce IRAK2 phosphorylation[35]. That report points out the possibility that IRAK2 is phosphorylated by IRAK1, thereby activating the intrinsic kinase activity of IRAK2. We have also shown here, by an *in vitro* kinase assay, that TLR2 stimulation induced phosphorylation of IRAK2 when cell lysates were immunoprecipitated with an IRAK2-specific antibody. Although it has been hypothesized that IRAK1 activates IRAK2 (ref. 35), there was TLR2-induced IRAK2 phosphorylation even in *Irak1*$^{-/Y}$ macrophages. These results indicate that IRAK1 is not responsible for the phosphorylation of IRAK2 in response to TLR stimulation. However, IRAK4 deficiency abrogated the phosphorylation of IRAK2, which suggests that activated IRAK4 phosphorylates IRAK1 and IRAK2, thereby inducing their autophosphorylation activity. Further, reconstitution of *Irak2*$^{-/-}$ macrophages with wild-type IRAK2 restored the phosphorylation of IRAK2 in response to MALP-2, but reconstitution with K237A IRAK2 did not, which indicates that the kinase activity of IRAK2 is critical for IRAK2 phosphorylation. It has also been reported that IRAK2 expression promotes the ubiquitination of TRAF6 (ref. 34). Thus, both IRAK1 and IRAK2 activate intracellular signaling cascades through TRAF6.

The requirement for the kinase activity of IRAK family members is still not well understood. Although we have shown here that IRAK4's kinase activity was critical for its function, IRAK1's kinase activity is reportedly dispensable for IL-1β-mediated signaling[37,40–43]. Furthermore, a kinase-defective IRAK1 mutant potently induced NF-κB activation. Reconstitution of *Irak2*$^{-/-}$ macrophages with wild-type IRAK2 restored IL-6 production in response to stimulation with MALP-2, but reconstitution with K237A IRAK2 did not, which suggests that IRAK2's kinase activity is essential for its function in regulating cytokine production.

It has been shown that IRAK1 is rapidly ubiquitinated and degraded by the ubiquitin-proteasome system after TLR stimulation[36]. IRAK1 is also reported to have 'PEST' sequences, which are involved in regulating proteolysis[16,44]. IRAK1 protein abundance and autophosphorylation were lower after TLR2 stimulation. In contrast, IRAK2 expression was not altered in response to TLR2 stimulation. Notably, IRAK2 autophosphorylation began 20 min after TLR2 stimulation, peaked at 8 h after stimulation and was sustained as late as 16 h after stimulation. Thus, IRAK2 may function exclusively to sustain TLR-mediated signaling and cause robust proinflammatory cytokine production.

The initial TLR2-induced expression of *Cxcl1* and *Tnfa* mRNA was lower in *Irak1*$^{-/Y}$ macrophages, although their expression was similar to the expression in wild-type cells at later time points. Those observations suggest that the presence of two kinases is beneficial for inducing strong initial cytokine responses to the invasion of pathogens. We speculate that the degradation of IRAK1 might be a prerequisite for preventing the overproduction of proinflammatory cytokines, which may cause harmful septic shock.

Among the IRAK family members, IRAK4 has been shown to be essential for the responses to TLR and IL-1R stimulation in *Irak4*$^{-/-}$ mice[17,19]. In response to TLR stimulation, IRAK4 phosphorylates IRAK1, inducing IRAK1 activation and an association between IRAK1 and TRAF6. Although IRAK1 is critical for IL-1R-mediated signaling in human embryonic kidney 293 cells lacking IRAK1 expression[35], analysis of *Irak1*$^{-/Y}$ mice shows that IRAK1 contributes modestly to TLR-induced cytokine production in macrophages[29,30], and the presence of IRAK1-independent signaling pathways has been predicted. We have shown here that TLR-mediated cytokine production was abrogated in the absence of both IRAK1 and IRAK2. Activation of MAP kinases was also abrogated when both IRAK1 and IRAK2 were absent. These results indicate that IRAK1 and IRAK2 function redundantly in the production of cytokines and MAP kinase activation. The phenotype of *Irak1*$^{-/Y}$*Irak2*$^{-/-}$ macrophages is reminiscent of that of *Irak4*$^{-/-}$ macrophages. It has been shown that IRAK4 phosphorylates IRAK1, thereby activating its kinase activity. Thus, it is plausible that IRAK2 is also phosphorylated by IRAK4, leading to its activation. Indeed, phosphorylation of IRAK2 has not been reported in *Irak4*$^{-/-}$ macrophages[22]. These results indicate that IRAK4 acts upstream of both IRAK1 and IRAK2 to activate downstream signaling cascades.

Our microarray analysis showed that IRAK1 and IRAK2 were critical for the regulation of only some MALP-2-inducible genes, although cytokines and chemokines are regulated by IRAK1 and

IRAK2. That result is consistent with the induction of NF-κB even in the absence of IRAK1 and IRAK2. A reported MyD88-dependent IRAK4 independent pathway[22] may be responsible for the expression of these genes. Identifying the signaling molecules responsible for the IRAK-independent signaling pathways will be essential for understanding complex TLR-induced gene expression mechanisms. However, the gene expression profiles of wild-type and *Irak2*$^{-/-}$ macrophages 2 h after stimulation with MALP-2 were similar. The expression of genes encoding cytokines was not sustained in *Irak2*$^{-/-}$ macrophages, and the expression of 38 genes was impaired 50% in *Irak2*$^{-/-}$ cells 8 h after stimulation. That result supports the idea that IRAK2 is involved in the expression of genes encoding cytokines later in response to the TLR stimulation. Further studies are needed to understand the mechanism underlying this signaling pathway.

Finally, our data have shown that IRAK1 and IRAK2 acted redundantly at early time points after TLR stimulation, whereas IRAK2 was critical for sustaining the responses at later time points. Both IRAK1 and IRAK2 seemed to be activated downstream of IRAK4. Moreover, the kinase activity of IRAK2 was essential for cytokine production in response to TLR stimulation in macrophages. Given that IRAK2 deficiency minimally affected TLR-induced gene expression, except for that of genes encoding proinflammatory cytokines, the development of a small molecule targeting IRAK2 kinase activity will be beneficial to therapies for septic shock by preventing a wide spectrum of immune suppression.

METHODS

Generation of *Irak2*$^{-/-}$ mice. *Irak2* was isolated from genomic DNA extracted from embryonic stem cells by PCR. The targeting vector was constructed by replacement of a 2.9-kilobase fragment encoding the *Irak2* open reading frame with a neomycin-resistance cassette and a herpes simplex virus thymidine kinase cassette driven by the promoter of the gene encoding phosphoglycerate kinase, which had been inserted into the genomic fragment for negative selection. After the targeting vector was transfected into embryonic stem cells, colonies doubly resistant to the aminoglycoside G418 and gancyclovir were selected and screened by PCR and their identities were further confirmed by Southern blot analysis. Homologous recombinants were microinjected into blastocysts from C57BL/6 female mice, and heterozygous F_1 progeny were intercrossed to obtain *Irak2*$^{-/-}$ mice. *Irak2*$^{-/-}$ mice on the 129/Sv × C57BL/6 background and their littermates (controls) were used. All animal experiments were with the approval of the Animal Research Committee of the Research Institute for Microbial Diseases (Osaka University).

Cells. Peritoneal exudate cells were isolated from the peritoneal cavities of mice 3 d after mice were injected with 2 ml of 4.0% (wt/vol) thioglycollate medium (Sigma) by washing with ice-cold Hank's buffered-salt solution (Invitrogen).

Reagents. MALP-2 was provided as described[45]. LPS from *Salmonella minnesota* Re-595 was from Sigma-Aldrich; poly(I:C) was from Amersham Biosciences; and R-848 was provided by the Pharmaceuticals and Biotechnology Laboratory of Japan Energy. CpG oligonucleotide was synthesized as described[46]. Polyclonal antibodies to phosphorylated Jnk (9251), p38 (9211) and Erk (9101) were from Cell Signaling. Polyclonal antibody to β-tubulin (anti-β-tubulin; sc-5274), anti-IκBα (sc-371), anti–NF-κB p50 (sc-1192) and anti–NF-κB p65 (sc-109) were from Santa Cruz. Rabbit polyclonal anti-IRAK1 and anti-IRAK4 were made as described[22,47]. Rabbit polyclonal anti-IRAK2 (3595) was from ProSci.

Measurement of cytokine production. Concentrations of cytokines in culture supernatants were measured by ELISA. ELISA kits for mouse TNF, IL-6 and KC were from R&D Systems.

***In vitro* kinase assay.** Peritoneal macrophages stimulated with MALP-2 (10 ng/ml) were lysed and immunoprecipitated with anti-IRAK1, anti-IRAK2 or anti-IRAK4, then the activity of IRAK1, IRAK2 and IRAK4 was measured by an *in vitro* kinase assay as described[22].

RNA hybridization. Peritoneal macrophages were treated for 0, 1, 2, 4 or 8 h with MALP-2 (10 ng/ml) and total RNA was extracted with TRIzol reagent (Invitrogen). RNA was separated by electrophoresis and transferred to nylon membranes and then hybridized with the appropriate cDNA probe. For the detection of *Irak2* mRNA expression, a 314–base pair fragment (nucleotides 894–1208) was used as a probe. The same membrane was rehybridized with an *Actb* probe (encoding β-actin) as a loading control.

Immunoblot analysis. Peritoneal macrophages were treated for various times with MALP-2 (10 ng/ml). Cells were then lysed in lysis buffer containing 1.0% (vol/vol) Nonidet-P40, 150 mM NaCl, 20 mM Tris-HCl, pH 7.5, 1 mM EDTA and a protease inhibitor 'cocktail' (Roche). Cell lysates were separated by SDS-PAGE and transferred to polyvinylidene difluoride membranes. Membranes were blotted with the appropriate specific antibodies and were visualized with an enhanced chemiluminescence system (NEN Life Science Products).

Electrophoretic mobility-shift assay. Nuclear extracts prepared from 4×10^6 peritoneal macrophages stimulated with MALP-2 (10 ng/ml) as described[12] were incubated with or without anti–NF-κB p65 or anti–NF-κB p50 and then were further incubated with a specific probe for NF-κB DNA-binding sites, separated by electrophoresis and visualized by autoradiography.

Construction of IRAK2 expression plasmids. Full-length IRAK2 cDNA was obtained by RT-PCR from a human cDNA library, and a point mutation resulting in a K237A substitution in the kinase domain was introduced by site-directed mutagenesis. Full-length or mutated IRAK2 cDNA was cloned into the 'LZR' vector.

Retroviral transduction. Highly efficient retroviral transduction of macrophages was achieved by transduction of hematopoietic stem cells before differentiation into macrophages as described[48]. Bone marrow was isolated from *Irak2*$^{-/-}$mice that had been injected intraperitoneally 4 d earlier with 5 mg of 5-fluorouracil (Nacalai Tesque). Cells were cultured in stem cell media (DMEM supplemented with 15% (vol/vol) FCS, sodium pyruvate (10 mM), L-glutamine (2 mM), β-mercaptoethanol (50 μM), penicillin (100 U/ml), streptomycin (100 g/ml), stem cell factor (100 ng/ml), IL-6 (10 ng/ml) and IL-3 (10 ng/ml)). Then, 48 h later, cells were transduced with retroviral supernatant (supplemented with stem cell factor, IL-6, IL-3 and 10 ng/ml of polybrene) on 2 successive days. Virus was produced with the PlatE retrovirus packaging cell line. After the second transduction, cells were washed and resuspended in macrophage growth media (RPMI 1640 medium supplemented with 10% (vol/vol) FCS, HEPES (10 mM), pH 7.0, sodium pyruvate (10 mM), L-glutamine (2 mM), β-mercaptoethanol (50 μM), penicillin (100 U/ml), streptomycin (100 g/ml) and macrophage colony–stimulating factor (40 ng/ml)). Cells were cultivated for 7 d and then analyzed.

Microarray. Peritoneal macrophages were stimulated for 0, 2, 4 or 8 h with MALP-2 (10 ng/ml), then total RNA was extracted with TRIzol (Invitrogen Life Technologies) and further purified with an RNeasy kit (Qiagen). Biotin-labeled cDNA was synthesized from 100 ng total RNA with the Ovation Biotin RNA Amplification and Labeling System (Nugen) according to the manufacturer's protocol. Affymetrix mouse Genome 430 2.0 microarray chips were hybridized, stained, washed and scanned according to the manufacturer's instructions. Data were analyzed MicroArray Suite software (Affymetrix) and ArrayAssist software (Stratagene).

Accession codes. UCSD-Nature Signaling Gateway (http://www.signaling-gateway.org): IRAK1 (A001277), IRAK2 (A001278), IRAKM and IRAK4 (A003450); GEO: microarray data, GSE10765.

Note: Supplementary information is available on the Nature Immunology website.

ACKNOWLEDGMENTS

We thank J.A. Thomas (University of Texas Southern Medical Center) for *Irak1*$^{-/Y}$ mice; all our colleagues in our laboratory; M. Hashimoto for secretarial assistance; and Y. Fujiwara, M. Shiokawa, A. Shibano and N. Kitagaki for technical assistance. Supported by the Ministry of Education, Culture, Sports,

Science, and Technology of Japan; the Ministry of Health, Labour and Welfare of Japan; the 21st Century Center of Excellence Program of Japan; and the National Institutes of Health (AI070167).

AUTHOR CONTRIBUTIONS

T. Kawagoe, O.T. and S.A. designed the research and analyzed data; T. Kawagoe did most of the experiments; S.S., K. Matsushita., H.K., K. Matsui., Y.K., T.S. and T.K. provided advice; and T. Kawagoe, O.T. and S.A. prepared the manuscript.

Published online at http://www.nature.com/natureimmunology
Reprints and permissions information is available online at http://npg.nature.com/reprintsandpermissions

1. Akira, S., Uematsu, S. & Takeuchi, O. Pathogen recognition and innate immunity. *Cell* **124**, 783–801 (2006).
2. Janeway, C.A., Jr. & Medzhitov, R. Innate immune recognition. *Annu. Rev. Immunol.* **20**, 197–216 (2002).
3. Beutler, B. Inferences, questions and possibilities in Toll-like receptor signalling. *Nature* **430**, 257–263 (2004).
4. Adachi, O. *et al.* Targeted disruption of the MyD88 gene results in loss of IL-1- and IL-18-mediated function. *Immunity* **9**, 143–150 (1998).
5. Kawai, T., Adachi, O., Ogawa, T., Takeda, K. & Akira, S. Unresponsiveness of MyD88-deficient mice to endotoxin. *Immunity* **11**, 115–122 (1999).
6. Fitzgerald, K.A. *et al.* Mal (MyD88-adapter-like) is required for Toll-like receptor-4 signal transduction. *Nature* **413**, 78–83 (2001).
7. Horng, T., Barton, G.M. & Medzhitov, R. TIRAP: an adapter molecule in the Toll signaling pathway. *Nat. Immunol.* **2**, 835–841 (2001).
8. Horng, T., Barton, G.M., Flavell, R.A. & Medzhitov, R. The adaptor molecule TIRAP provides signalling specificity for Toll-like receptors. *Nature* **420**, 329–333 (2002).
9. Yamamoto, M. *et al.* Essential role for TIRAP in activation of the signalling cascade shared by TLR2 and TLR4. *Nature* **420**, 324–329 (2002).
10. Hoebe, K. *et al.* Identification of Lps2 as a key transducer of MyD88-independent TIR signalling. *Nature* **424**, 743–748 (2003).
11. Oshiumi, H., Matsumoto, M., Funami, K., Akazawa, T. & Seya, T. TICAM-1, an adaptor molecule that participates in Toll-like receptor 3-mediated interferon-β induction. *Nat. Immunol.* **4**, 161–167 (2003).
12. Yamamoto, M. *et al.* Role of adaptor TRIF in the MyD88-independent toll-like receptor signaling pathway. *Science* **301**, 640–643 (2003).
13. Kagan, J.C. *et al.* TRAM couples endocytosis of Toll-like receptor 4 to the induction of interferon-β. *Nat. Immunol.* **9**, 361–368 (2008).
14. Fitzgerald, K.A. *et al.* LPS-TLR4 signaling to IRF-3/7 and NF-κB involves the toll adapters TRAM and TRIF. *J. Exp. Med.* **198**, 1043–1055 (2003).
15. Yamamoto, M. *et al.* TRAM is specifically involved in the Toll-like receptor 4-mediated MyD88-independent signaling pathway. *Nat. Immunol.* **4**, 1144–1150 (2003).
16. Janssens, S. & Beyaert, R. Functional diversity and regulation of different interleukin-1 receptor-associated kinase (IRAK) family members. *Mol. Cell* **11**, 293–302 (2003).
17. Suzuki, N. *et al.* Severe impairment of interleukin-1 and Toll-like receptor signalling in mice lacking IRAK-4. *Nature* **416**, 750–756 (2002).
18. Suzuki, N. *et al.* IL-1R-associated kinase 4 is required for lipopolysaccharide-induced activation of APC. *J. Immunol.* **171**, 6065–6071 (2003).
19. Honda, K. *et al.* Role of a transductional-transcriptional processor complex involving MyD88 and IRF-7 in Toll-like receptor signaling. *Proc. Natl. Acad. Sci. USA* **101**, 15416–15421 (2004).
20. Koziczak-Holbro, M. *et al.* IRAK-4 kinase activity is required for interleukin-1 (IL-1) receptor- and toll-like receptor 7-mediated signaling and gene expression. *J. Biol. Chem.* **282**, 13552–13560 (2007).
21. Kim, T.W. *et al.* A critical role for IRAK4 kinase activity in Toll-like receptor-mediated innate immunity. *J. Exp. Med.* **204**, 1025–1036 (2007).
22. Kawagoe, T. *et al.* Essential role of IRAK-4 protein and its kinase activity in Toll-like receptor-mediated immune responses but not in TCR signaling. *J. Exp. Med.* **204**, 1013–1024 (2007).
23. Picard, C. *et al.* Pyogenic bacterial infections in humans with IRAK-4 deficiency. *Science* **299**, 2076–2079 (2003).
24. Medvedev, A.E. *et al.* Cutting edge: expression of IL-1 receptor-associated kinase-4 (IRAK-4) proteins with mutations identified in a patient with recurrent bacterial infections alters normal IRAK-4 interaction with components of the IL-1 receptor complex. *J. Immunol.* **174**, 6587–6591 (2005).
25. Yang, K. *et al.* Human TLR-7-, -8-, and -9-mediated induction of IFN-α/β and -λ is IRAK-4 dependent and redundant for protective immunity to viruses. *Immunity* **23**, 465–478 (2005).
26. Ku, C.L. *et al.* Selective predisposition to bacterial infections in IRAK-4-deficient children: IRAK-4-dependent TLRs are otherwise redundant in protective immunity. *J. Exp. Med.* **204**, 2407–2422 (2007).
27. Kobayashi, K. *et al.* IRAK-M is a negative regulator of Toll-like receptor signaling. *Cell* **110**, 191–202 (2002).
28. Croston, G.E., Cao, Z. & Goeddel, D.V. NF-κB activation by interleukin-1 (IL-1) requires an IL-1 receptor-associated protein kinase activity. *J. Biol. Chem.* **270**, 16514–16517 (1995).
29. Kanakaraj, P. *et al.* Interleukin (IL)-1 receptor-associated kinase (IRAK) requirement for optimal induction of multiple IL-1 signaling pathways and IL-6 production. *J. Exp. Med.* **187**, 2073–2079 (1998).
30. Thomas, J.A. *et al.* Impaired cytokine signaling in mice lacking the IL-1 receptor-associated kinase. *J. Immunol.* **163**, 978–984 (1999).
31. Uematsu, S. *et al.* Interleukin-1 receptor-associated kinase-1 plays an essential role for Toll-like receptor (TLR)7- and TLR9-mediated interferon-α induction. *J. Exp. Med.* **201**, 915–923 (2005).
32. Muzio, M., Ni, J., Feng, P. & Dixit, V.M. IRAK (Pelle) family member IRAK-2 and MyD88 as proximal mediators of IL-1 signaling. *Science* **278**, 1612–1615 (1997).
33. Hardy, M.P. & O'Neill, L.A. The murine IRAK2 gene encodes four alternatively spliced isoforms, two of which are inhibitory. *J. Biol. Chem.* **279**, 27699–27708 (2004).
34. Keating, S.E., Maloney, G.M., Moran, E.M. & Bowie, A.G. IRAK-2 participates in multiple toll-like receptor signaling pathways to NFκB via activation of TRAF6 ubiquitination. *J. Biol. Chem.* **282**, 33435–33443 (2007).
35. Wesche, H. *et al.* IRAK-M is a novel member of the Pelle/interleukin-1 receptor-associated kinase (IRAK) family. *J. Biol. Chem.* **274**, 19403–19410 (1999).
36. Yamin, T.T. & Miller, D.K. The interleukin-1 receptor-associated kinase is degraded by proteasomes following its phosphorylation. *J. Biol. Chem.* **272**, 21540–21547 (1997).
37. Li, X. *et al.* Mutant cells that do not respond to interleukin-1 (IL-1) reveal a novel role for IL-1 receptor-associated kinase. *Mol. Cell. Biol.* **19**, 4643–4652 (1999).
38. Swantek, J.L., Tsen, M.F., Cobb, M.H. & Thomas, J.A. IL-1 receptor-associated kinase modulates host responsiveness to endotoxin. *J. Immunol.* **164**, 4301–4306 (2000).
39. Li, S., Strelow, A., Fontana, E.J. & Wesche, H. IRAK-4: a novel member of the IRAK family with the properties of an IRAK-kinase. *Proc. Natl. Acad. Sci. USA* **99**, 5567–5572 (2002).
40. Knop, J. & Martin, M.U. Effects of IL-1 receptor-associated kinase (IRAK) expression on IL-1 signaling are independent of its kinase activity. *FEBS Lett.* **448**, 81–85 (1999).
41. Maschera, B., Ray, K., Burns, K. & Volpe, F. Overexpression of an enzymically inactive interleukin-1-receptor-associated kinase activates nuclear factor-κB. *Biochem. J.* **339**, 227–231 (1999).
42. Li, X., Commane, M., Jiang, Z. & Stark, G.R. IL-1-induced NFκB and c-Jun N-terminal kinase (JNK) activation diverge at IL-1 receptor-associated kinase (IRAK). *Proc. Natl. Acad. Sci. USA* **98**, 4461–4465 (2001).
43. Jensen, L.E. & Whitehead, A.S. IRAK1b, a novel alternative splice variant of interleukin-1 receptor-associated kinase (IRAK), mediates interleukin-1 signaling and has prolonged stability. *J. Biol. Chem.* **276**, 29037–29044 (2001).
44. Rechsteiner, M. & Rogers, S.W. PEST sequences and regulation by proteolysis. *Trends Biochem. Sci.* **21**, 267–271 (1996).
45. Takeuchi, O. *et al.* Cutting edge: preferentially the R-stereoisomer of the mycoplasmal lipopeptide macrophage-activating lipopeptide-2 activates immune cells through a toll-like receptor 2- and MyD88-dependent signaling pathway. *J. Immunol.* **164**, 554–557 (2000).
46. Hemmi, H. *et al.* Toll-like receptor recognizes bacterial DNA. *Nature* **408**, 740–745 (2000).
47. Sato, S. *et al.* A variety of microbial components induce tolerance to lipopolysaccharide by differentially affecting MyD88-dependent and -independent pathways. *Int. Immunol.* **14**, 783–791 (2002).
48. Barton, G.M., Kagan, J.C. & Medzhitov, R. Intracellular localization of Toll-like receptor 9 prevents recognition of self DNA but facilitates access to viral DNA. *Nat. Immunol.* **7**, 49–56 (2006).

Available online at www.sciencedirect.com
ScienceDirect
Current Opinion in Immunology

MDA5/RIG-I and virus recognition

Osamu Takeuchi and Shizuo Akira

The innate immune system initially recognizes RNA virus infection and evokes antiviral responses by producing type I interferons (IFNs). Toll-like receptors (TLRs) and cytoplasmic retinoic acid-inducible gene I (RIG-I)-like helicases (RLHs) are the two major receptor systems for detecting RNA viruses. The RLH signaling pathways play essential roles in the recognition of RNA viruses in various cells, with the exception of plasmacytoid dendritic cells, which utilize TLRs for virus recognition. The route of infection determines the cell types responsible for type I IFN production. Recent studies have suggested that TLRs are critical for activation of adaptive immune responses against several virus infections, although it may be premature to draw such a conclusion for virus infections in general. In this review, we will discuss recent advances toward clarifying the signaling pathways activated by RLHs and TLRs.

Addresses
Laboratory of Host Defense, WPI Immunology Frontier Research Center, Osaka University, 3-1 Yamada-oka, Suita, Osaka 565-0871, Japan

Corresponding author: Akira, Shizuo (sakira@biken.osaka-u.ac.jp)

Current Opinion in Immunology 2008, **20**:17–22

This review comes from a themed issue on
Innate Immunity
Edited by Wayne Yokayama and Marco Colonna

0952-7915/$ – see front matter
Published by Elsevier Ltd.

DOI 10.1016/j.coi.2008.01.002

Introduction

Innate immunity is characterized by the use of germline-encoded pattern recognition receptors (PRRs) to sense components specific to micro-organisms [1–3]. Recent studies have identified three major classes of PRRs, designated Toll-like receptors (TLRs), retinoic acid-inducible gene I (RIG-I)-like helicases (RLHs) and nucleotide-oligomerization domain (NOD)-like receptors (NLRs). In response to virus infections, viral components such as RNA and DNA are recognized by TLRs and RLHs, and cells are activated to produce type I interferons (IFNs) and proinflammatory cytokines. Type I IFNs, comprised of multiple IFN-α isoforms and a single IFN-β, and other members, such as IFN-ω, IFN-ε and IFN-κ, are pleiotropic cytokines that are essential for antiviral immune responses [4]. They induce apoptosis of virus-infected cells and cellular resistance to virus infection, as well as activating natural killer (NK) and T cells.

TLRs are comprised of leucine-rich repeats (LRRs), a transmembrane domain and a cytoplasmic Toll/interleukin 1 receptor (IL-1R) homology (TIR) domain [1]. Among the 13 TLRs identified in mammals, TLR3, TLR7, TLR8 and TLR9 are involved in the recognition of microbial nucleotides. These TLRs are expressed on the surface of cytoplasmic vesicles such as endosomes and the endoplasmic reticulum with the LRR domain in the vesicular space. TLR3 detects double-stranded (ds) RNA, while TLR7 and TLR8 recognize single-stranded (ss) RNA and TLR9 recognizes unmethylated DNA with CpG motifs. TLR-mediated signaling pathways recruit TIR domain-containing adaptors such as MyD88 and TIR domain-containing adaptor inducing IFN-β (TRIF), thereby leading to the activation of transcription factors such as nuclear factor-κB (NF-κB) and IFN-regulatory factors (IRFs), which regulate the expression of genes that encode proinflammatory cytokines and type I IFNs, respectively. Since TLRs are transmembrane proteins, they are not able to detect viral components present in the cytoplasm of a cell.

RIG-I (also known as DDX58) was identified as a candidate for a cytoplasmic viral RNA detector [5]. RIG-I is comprised of two N-terminal caspase-recruitment domains (CARDs) followed by a DExD/H box RNA helicase domain. RIG-I forms the RLH family together with melanoma differentiation-associated gene 5 (MDA5; also known as helicard or IFIH1) and LGP2 based on the high similarities among their helicase domains [6,7]. The helicase domains of RLH family members are highly similar to that of mammalian Dicer. The expression of genes encoding RLHs is strongly induced by IFNs. RLHs interact with dsRNAs through their helicase domain, and dsRNA stimulation induces their ATP catalytic activity. A C-terminal portion of RIG-I, designated the repressor domain (RD), was shown to inhibit the triggering of RIG-I signaling in the steady state [8]. The N-terminal CARDs are responsible for activating downstream signaling pathways that mediate dsRNA-induced type I IFN production.

In this review, we will describe the functions and signaling pathways of RLHs, and discuss the relationships among RLHs and TLRs in antiviral immune responses.

Recognition of RNA viruses by RLHs

RNA virus infections generate dsRNA for virus replication in infected cells. Initially, both RIG-I and MDA5 were implicated in the recognition of polyinosinic polycytidylic acid (poly I:C), a synthetic analogue of viral dsRNA. However, analysis of RIG-I$^{-/-}$ and MDA5$^{-/-}$

mice revealed that MDA5, but not RIG-I, was responsible for the response to poly I:C stimulation [9••,10]. On the other hand, RIG-I, but not MDA5, recognizes 5′-triphosphate ssRNA synthesized by T7 polymerase *in vitro* [11••,12••]. RNAs from some viruses are 5′-triphosphorylated and uncapped, whereas the 5′ ends of host mRNAs are capped. Thus, RIG-I discriminates virus and host RNAs based on the differences in the 5′ ends of their RNAs.

RNA viruses are also differentially recognized by RIG-I and MDA5. RIG-I$^{-/-}$ cells do not produce type I IFNs in response to various RNA viruses, including paramyxoviruses, vesicular stomatitis virus (VSV) and influenza virus [9••,13]. By contrast, MDA5$^{-/-}$ cells do not respond to infection with picornaviruses such as encephalomyocarditis virus (EMCV) and Theiler's virus. Cells infected with EMCV, but not influenza virus, generate dsRNA [12••]. Dephosphorylation of 5′-triphosphate RNA or the influenza genome results in a loss of their ability to induce IFNs, suggesting that recognition by RIG-I is mediated through 5′-triphosphate ssRNA. Consistent with defects in type I IFN production, RIG-I$^{-/-}$ and MDA5$^{-/-}$ mice are highly susceptible to inoculation with VSV and EMCV, respectively [9••]. Japanese encephalitis virus and hepatitis C virus, which both belong to the Flaviviridae family, are recognized by RIG-I. However, Dengue virus and West Nile virus, which also belong to the Flaviviridae family, were reported to induce type I IFN production even in the absence of either RIG-I or MDA5 [9••,14–16]. Furthermore, siRNA experiments suggested that Dengue virus was recognized by a combination of RIG-I and MDA5.

RIG-I-mediated signaling is positively and negatively controlled by ubiquitination of RIG-I. First, the CARDs of RIG-I undergo Lys 63-linked ubiquitination by tripartite motif (TRIM) 25, a ubiquitin E3 ligase composed of a RING finger domain, a B box/coiled-coil domain and a SPRY domain [17•]. This ubiquitination is necessary for efficient activation of the RIG-I signaling pathway, and TRIM25$^{-/-}$ cells display impaired production of type I IFNs against viral infection. On the other hand, RIG-I also undergoes ubiquitination by the ubiquitin ligase RNF125, which leads to its proteasomal degradation [18]. Thus, RIG-1 ubiquitination by RNF125 is considered to inhibit aberrant activation of RIG-I signaling.

RNase L, an endonuclease originally thought to cleave viral ssRNA, was reported to be involved in the production of IFN-β in response to RNA virus infection or dsRNA stimulation [19]. Briefly, 2′,5′-linked oligoadenylate generated by virus infection activates RNase L to cleave self RNA, resulting in the generation of small RNA products. These small RNAs are responsible for RIG-I/MDA5-mediated recognition and subsequent production of type I IFNs. However, the precise structures of the RNAs generated by RNase L that are recognized by RIG-I/MDA5 need to be further investigated.

Since LGP2 lacks a CARD, it is suggested to function as a negative regulator of RIG-I/MDA5 signaling. Overexpression of LGP2 inhibits Sendai virus and Newcastle disease virus (NDV) signaling [6–8]. LGP2 also contains an RD, and this RD was found to interact with the RD of RIG-I and suppress its self-association. Recently, Lgp2$^{-/-}$ mice were generated and analyzed by Barber and coworkers [20]. Lgp2$^{-/-}$ mice show highly elevated induction of type I IFNs in response to poly I:C stimulation, and modestly increased IFN production in response to VSV infection. On the other hand, Lgp2$^{-/-}$ mice exhibit partially impaired type I IFN production in response to EMCV infection. The authors proposed that LGP2 is a negative regulator of RIG-I, but not of MDA5. However, given that both poly I:C and EMCV are recognized by MDA5, the difference cannot be simply explained by differential usage of LGP2 for RIG-I and MDA5 signaling.

The RLH signaling pathway

The CARDs of RIG-I and MDA5 are responsible for initiating signaling cascades (Figure 1). RIG-I and MDA5 associate with an adaptor protein, IFN-β promoter stimulator 1 (IPS-1; also known as MAVS, VISA or CARDIF), which also contains a CARD [21–24]. Overexpression of IPS-1 induces the activation of IFN gene promoters as well as NF-κB. IPS-1$^{-/-}$ mice are defective in producing type I IFNs and proinflammatory cytokines in response to all RNA viruses recognized by either RIG-I or MDA5 [25,26]. These findings indicate that IPS-1 plays an essential role in RIG-I/MDA5 signaling. Interestingly, this protein is present in the outer mitochondrial membrane, suggesting that mitochondria may be important for IFN responses, in addition to their roles in metabolism and cell death [22]. Recently, IPS-1 and RIG-I were found to associate with Atg5–Atg12 conjugates, which are essential components for autophagy [27]. Atg5$^{-/-}$ mouse embryonic fibroblasts show increased type I IFN production in response to RNA virus infection, suggesting that the autophagic machinery directly affects the RIG-I signaling pathway in addition to autophagosome formation.

IPS-1 was found to associate with TNF-receptor-associated factor (TRAF) 3, an E3 ubiquitin ligase assembling lysine 63-linked polyubiquitin chains, through its C-terminal TRAF domain [28–30]. TRAF3$^{-/-}$ cells show severely impaired production of type I IFNs in response to virus infection. Recently, a deubiquitinase named DUBA was shown to deubiquitinate TRAF3 and suppress RLH signaling [31•]. TRAF3 recruits and activates two IKK-related kinases, designated TANK-binding kinase 1 (TBK1) and inducible IκB kinase (IKK-*i*; also known as IKKε), which phosphorylate IRF-3 and IRF-7